

## Supporting Information

### Isostructural Self-assembly of 2'-Deoxyguanosine Derivatives in Aqueous and Organic Media

Marilyn García-Arriaga, Gerard Hobley and José M. Rivera\*<sup>a</sup>

College of Natural Sciences, Department of Chemistry, University of Puerto Rico, Río Piedras Campus, San Juan, PR, 00931. Fax: 787-756-8242; Tel: 787-764-0000, ext. 2906; E-mail: jmrivortz@mac.com

#### Table of contents

|  |            |
|--|------------|
| <b>General Experimental Procedures</b>                   | <b>S2</b>  |
| <b>Characterization and Instrumentation</b>              | <b>S3</b>  |
| <b>General method for esterifications</b>                | <b>S3</b>  |
| <b>General Method for the Azide/Alkyne Cycloaddition</b> | <b>S5</b>  |
| <b>Circular Dichroism (CD) Spectroscopy</b>              | <b>S20</b> |
| <b>Self-assembly studies</b>                             | <b>S20</b> |
| <b>Diffusion NMR studies</b>                             | <b>S30</b> |
| <b>Variable temperature NMR</b>                          | <b>S33</b> |
| <b>Differential Scanning Calorimetry (DSC)</b>           | <b>S34</b> |
| <b>References</b>  | <b>S35</b> |

#### Table of Figures

|   |            |
|---|------------|
| <b>Scheme S1.</b> Synthesis of <b>mAGcat</b> and <b>dGcat</b>                           | <b>S3</b>  |
| <b>Figure S1.</b> <sup>1</sup> H-NMR of <b>dGhaz</b> , in DMSO- <i>d</i> <sub>6</sub>   | <b>S7</b>  |
| <b>Figure S2.</b> <sup>13</sup> C-NMR of <b>dGhaz</b> , in DMSO- <i>d</i> <sub>6</sub>  | <b>S8</b>  |
| <b>Figure S3.</b> COSY of <b>dGhaz</b> , in DMSO- <i>d</i> <sub>6</sub>                 | <b>S9</b>  |
| <b>Figure S4.</b> <sup>1</sup> H-NMR of <b>mAGcat</b> , in DMSO- <i>d</i> <sub>6</sub>  | <b>S10</b> |
| <b>Figure S5.</b> <sup>13</sup> C-NMR of <b>mAGcat</b> , in DMSO- <i>d</i> <sub>6</sub> | <b>S11</b> |
| <b>Figure S6.</b> COSY of <b>mAGcat</b> , in DMSO- <i>d</i> <sub>6</sub>                | <b>S12</b> |

|   |     |
|---|-----|
| <b>Figure S7.</b> HMBC of <b>mAGcat</b> , in DMSO- <i>d</i> <sub>6</sub>                          | S13 |
| <b>Figure S8.</b> NOESY of <b>mAGcat</b> , in DMSO- <i>d</i> <sub>6</sub>                         | S14 |
| <b>Figure S9.</b> <sup>1</sup> H-NMR of <b>dGcat</b> , in DMSO- <i>d</i> <sub>6</sub>             | S15 |
| <b>Figure S10.</b> <sup>13</sup> C-NMR of <b>dGcat</b> , in DMSO- <i>d</i> <sub>6</sub>           | S16 |
| <b>Figure S11.</b> COSY of <b>dGcat</b> , in DMSO- <i>d</i> <sub>6</sub>                          | S17 |
| <b>Figure S12.</b> HMBC of <b>dGcat</b> , in DMSO- <i>d</i> <sub>6</sub>                          | S18 |
| <b>Figure S13.</b> NOESY of <b>dGcat</b> , in DMSO- <i>d</i> <sub>6</sub>                         | S19 |
| <b>Figure S14.</b> CD spectra of <b>mAGi</b> and <b>mAGcat</b>                                    | S20 |
| <b>Figure S15.</b> <sup>1</sup> H-NMR of <b>mAGcat</b> , in H <sub>2</sub> O-D <sub>2</sub> O     | S21 |
| <b>Figure S16.</b> <sup>1</sup> H-NMR of <b>mAGcat</b> and <b>mAGi</b>                            | S22 |
| <b>Figure S17.</b> Titration of <b>mAGcat</b>   | S23 |
| <b>Figure S18.</b> <sup>1</sup> H-NMR of <b>dGcat</b> , in H <sub>2</sub> O-D <sub>2</sub> O      | S24 |
| <b>Figure S19.</b> COSY of <b>mAGcat</b> , in D <sub>2</sub> O                                    | S25 |
| <b>Figure S20.</b> NOESY of <b>mAGcat</b> , in D <sub>2</sub> O                                   | S26 |
| <b>Figure S21.</b> Expansion of the NOESY of <b>mAGcat</b> , in D <sub>2</sub> O                  | S27 |
| <b>Figure S22.</b> NOESY of <b>mAGcat</b> , in H <sub>2</sub> O-D <sub>2</sub> O                  | S28 |
| <b>Figure S23.</b> Expansion of the NOESY of <b>mAGcat</b> , in H <sub>2</sub> O-D <sub>2</sub> O | S29 |
| <b>Figure S24.</b> Detailed explanation of the connectivities shown in Figure 2a                  | S30 |
| <b>Figure S25.</b> DOSY of <b>mAGcat</b> , in D <sub>2</sub> O                                    | S32 |
| <b>Figure S26.</b> Theoretical hydrodynamic radius of <b>mAGcat</b>                               | S33 |
| <b>Figure S27.</b> NMR melting curves of <b>mAGcat</b> and <b>mAGi</b>                            | S34 |
| <b>Figure S28.</b> Variable temperature <sup>1</sup> H-NMR of <b>mAGcat</b>                       | S34 |
| <b>Figure S29.</b> DSC melting curve of <b>mAGcat</b> in H <sub>2</sub> O                         | S35 |

### **General Experimental Procedures**

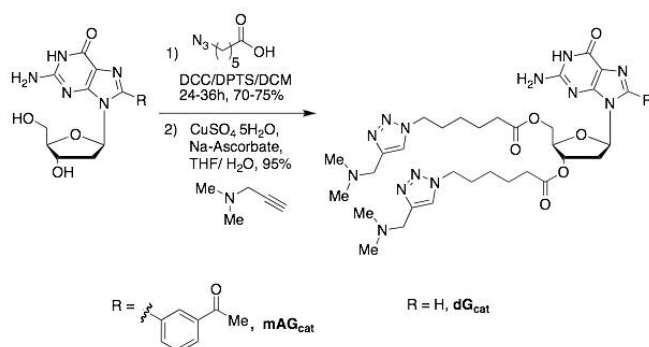
Dimethylformamide (DMF) was purchased anhydrous from Aldrich and used without further treatment. MeOH (1.00 L) was distilled from Magnesium (5.00g) and iodine (500 mg). Unless specified, all other reagents and solvents were obtained from commercial sources and use without further purification. 8-(3-acetylphenyl)-2'-deoxyguanosine was synthesized according to the procedures outlined elsewhere.<sup>1</sup> Column chromatography was performed using silica gel 60, 44-63 μm from Sorbent Technologies. For TLC, EMD

silica gel 60 F<sub>254</sub> glass backed plates from Sorbent Technologies, were used. Visualization of TLC plates was effected with UV light or anisaldehyde as a stain. Reactions requiring anhydrous conditions were carried out using oven or flame-dried glassware under Argon.

### **Characterization and Instrumentation**

NMR spectra were recorded on Bruker DRX-500 or AV-500 spectrometer, with nominal frequencies of 500.13 MHz for proton and 125 MHz and for carbon respectively. All NMR experiments were performed at 298 K unless otherwise stated. All compounds were characterized with <sup>1</sup>H, <sup>13</sup>C NMR and 2D-NMR techniques such as COSY, HMBC and NOESY. All chemical shifts are reported in parts per million relative to the residual undeuterated solvent as an internal reference. The following abbreviations are used to explain the multiplicities: s, singlet; d, doublet; t, triplet; q, quartet; m, multiple; b, broad. The FT-IR analyses were performed on a Bruker Tensor 27 spectrophotometer equipped with Helios Attenuated Total Reflectance (ATR) with a diamond crystal. CD spectra were acquired on an OLIS DSM-10 UV-Vis CD or a Jasco 710 spectrophotometer. DSC analyses were performed on a VP-DSC from MicroCal and Origin (v. 7) was use for data processing. Melting temperatures were determined using Fisher brand electro-thermal digital melting point apparatus from Fisher Scientific. Mass Spectroscopy was recorded in a Micromass Quattro Micro API triple quadrupole mass spectrometer with an ESI source (Micromass, Inc., Manchester, UK).

### **General method for esterifications using 8-(3-acetylphenyl)-2'-deoxyguanosine as an example**



**Scheme S1.** Synthesis of **mAGcat** and **dGcat**.

8-(3-acetylphenyl)-2'-deoxyguanosine was suspended in anhydrous DMF (20 mg mL<sup>-1</sup>). To this suspension, a 1:1 complex of 4-dimethylaminopyridine: 4-toluenesulphonic acid<sup>2</sup> (DPTS) (0.5 equivalents), 6-azidohexanoic acid<sup>3</sup> (2.5 equivalents) and dicyclohexylcarbodiimide (2.5 equivalents) were added. The reaction mixture was stirred until TLC (CHCl<sub>3</sub>-MeOH, 80:20) showed complete conversion of the starting material. The reaction mixture was quenched by the addition of an excess of MeOH and this was followed by solvent evaporation. The resulting solid material was dissolved in EtOAc and washed with 10% NaHCO<sub>3</sub> (2 × 25 mL) and brine (1 × 25 mL). The organic phase was separated, dried over MgSO<sub>4</sub> and adsorbed directly onto silica gel. Dry loading of the silica onto a chromatography column followed by chromatography (MeOH-CHCl<sub>3</sub>, 1:19) afforded the target compound as a foam.

**8-(3-Acetylphenyl)-(3',5'-bis-O-(6-azidohexanoyloxy))-2'-deoxyguanosine.**

**(mAGhaz):** Light yellow foam (85 % yield). <sup>1</sup>H NMR (500 MHz, DMSO-*d*<sub>6</sub>): δ 10.83 (s, 1H), 8.20 (s, 1H), 8.07 (d, *J* = 7.5 Hz, 1H), 7.87 (d, *J* = 7.5 Hz, 1H), 7.69 (t, *J* = 8.2 Hz, 1H), 6.50 (b s, 2H), 6.10 (t, *J* = 7.1 Hz, 1H), 5.44 (m, 1H), 4.43 (dd, *J* = 5.1, 12.2 Hz, 1H), 4.27 (dd, *J* = 7.5, 11.5 Hz, 1H), 4.15 (b m, 1H), 3.51 (m, 1H), 3.27 (q, *J* = 7.0 Hz, 4H), 2.63 (s, 3H), 2.35 (m, 1H), 2.30 (q, *J* = 7.5 Hz, 4H), 1.52 (m, 8H), 1.30 (m, 4H). <sup>13</sup>C NMR (125 MHz, DMSO-*d*<sub>6</sub>): δ 198.1, 173.3, 173.0, 157.3, 153.8, 152.7, 146.8, 137.8, 134.0, 131.2, 129.8, 129.6, 129.5, 117.9, 85.4, 82.4, 75.3, 64.2, 51.1, 34.5, 34.0, 33.9, 28.5, 27.7, 26.2, 24.5. IR (ν<sub>max</sub>): 3324, 2928, 2850, 2091, 1734, 1684, 1624, 1570, 1242, 1087, 640 cm<sup>-1</sup>. ESI-MS *m/z* 664.53 [M+H]<sup>+</sup>.

**(3',5'-bis-O-(6-azidohexanoyloxy))-2'-deoxyguanosine. (dGhaz):** Ivory solid (52 % yield). Mp 153-155 °C. <sup>1</sup>H NMR (500 MHz, DMSO-*d*<sub>6</sub>): δ 10.71 (s, 1H), 7.91 (s, 1H), 6.51 (s, 2H), 6.13 (t, *J* = 5.0 Hz, 1H), 5.32 (d, *J* = 5.0 Hz, 1H), 4.22 (m, 3H), 3.32 (t, *J* = 10.0 Hz, 2H), 3.28 (t, *J* = 10.0 Hz, 2H), 2.92 (m, 1H), 2.45 (m, 1H), 2.35 (m, 4H), 1.53 (m, 8H), 1.32 (m, 4H). <sup>13</sup>C NMR (125 MHz, DMSO-*d*<sub>6</sub>): δ 172.6, 172.4, 156.8, 153.8, 151.1, 135.2, 116.8, 82.7, 81.6, 74.4, 63.5, 50.5, 35.6, 33.3, 33.1, 28.0, 27.9, 25.6, 23.9,

23.8. IR ( $\nu_{\max}$ ): 3392, 3315, 3169, 2731, 2090, 1715, 1594, 1168, 1101, 943  $\text{cm}^{-1}$ . ESI-MS  $m/z$  546.60  $[\text{M}+\text{H}]^+$ . (**Figure S1-3**)

**General Method for the Azide/Alkyne Cycloaddition Catalyzed by  $\text{CuSO}_4$  and Sodium Ascorbate using  $\text{mAG}_{\text{haz}}$  as an example.**

The starting material,  $\text{mAG}_{\text{haz}}$  (417 mg, 626  $\mu\text{mol}$ ) and 1-dimethylamino-2-propyne (156 mg, 200  $\mu\text{L}$ , 1.88 mmol) were dispersed in THF: 100 mM sodium phosphate buffer (pH 7.01) (3:1, 40.0 mL). To this was added sodium ascorbate (37.2 mg, 188  $\mu\text{mol}$ , 30 mol %) and then  $\text{CuSO}_4$  (626  $\mu\text{L}$  of a 100 mM solution, 62.6  $\mu\text{mol}$ , 10 mol %). When the starting material was consumed as determined by TLC (1:9, MeOH- $\text{CHCl}_3$ ) the solvent was removed under reduced pressure then dispersed in chloroform and loaded onto a chromatography column. The product was eluted using a gradient of MeOH- $\text{CHCl}_3$  (1:19) to  $\text{Et}_3\text{N}$ -MeOH- $\text{CHCl}_3$  (1:1:18). The oil thus obtained was dispersed dichloromethane (DCM), precipitated onto the walls of a round bottomed flask by adding  $\text{Et}_2\text{O}$ , the  $\text{Et}_2\text{O}$ -DCM decanted off and the residue dried under reduced pressure. This process was repeated until a pale yellow foam was obtained.

**(8-(3-acetylphenyl)-2-amino-6-oxo-1H-purin-9(6H)-yl)-2-((6-(4-((dimethylamino)methyl)-1H-1,2,3-triazol-1-yl)hexanoyloxy)methyl)tetrahydrofuran-3-yl 6-(4-((dimethylamino)methyl)-1H-1,2,3-triazol-1-yl)hexanoate ( $\text{mAG}_{\text{cat}}$ ).** Light yellow foam (61% yield).  $^1\text{H}$  NMR (500 MHz,  $\text{DMSO}-d_6$ ):  $\delta$  10.89 (s, 1H), 8.20 (s, 1H), 8.07 (d,  $J = 7.5$  Hz, 1H), 7.93 (d,  $J = 4.5$  Hz, 2H), 7.89 (d,  $J = 7.5$  Hz, 1H), 7.69 (t,  $J = 7.5$  Hz, 1H), 6.54 (s, 1H), 6.10 (t,  $J = 6.5$  Hz, 1H), 5.43 (s, 1H), 4.42 (m, 1H), 4.26 (q,  $J = 6.5$  Hz, 1H), 4.14 (s, 1H), 3.53 (m, 1H), 3.45 (d,  $J = 11.0$  Hz, 4H), 2.63 (s, 3H), 2.35 (m, 1H), 2.26 (q,  $J = 7.0$  Hz, 4H), 2.11 (s, 12H), 1.76 (m, 4H), 1.48 (m, 4H), 1.19 (m, 4H).  $^{13}\text{C}$  NMR (125 MHz,  $\text{DMSO}-d_6$ ):  $\delta$  197.5, 172.6, 172.3, 156.7, 153.2, 152.0, 146.1, 143.6, 143.5, 137.1, 133.3, 129.2, 128.8, 123.5, 117.2, 84.7, 81.7, 74.6, 63.6, 53.6, 53.6, 49.0, 44.5, 33.1, 29.3, 25.2, 23.7, 23.6. IR ( $\nu_{\max}$ ): 3317, 2941, 1732, 1597, 1358, 1250, 1172  $\text{cm}^{-1}$ . ESI-MS  $m/z$  830.9  $[\text{M}+\text{H}]^+$ . (**Figure S4-8**)

**2-amino-6-oxo-1H-purin-9(6H)-yl)-2-((6-(4-((dimethylamino)methyl)-1H-1,2,3-triazol-1-yl) hexanoyloxy)methyl)tetrahydrofuran-3-yl 6-(4-((dimethylamino)**

**methyl)-1H-1,2,3-triazol-1-yl)hexanoate (dGcat).** Light yellow solid (66 % yield). Mp 52-55 °C. <sup>1</sup>H NMR (500 MHz, DMSO-*d*<sub>6</sub>): δ 10.76 (s, 1H), 7.98 (d, *J* = 5.0 Hz, 2H), 7.93 (s, 1H), 6.56 (s, 2H), 6.13 (t, *J* = 10.0 Hz, 1H), 5.31 (s, 1H), 4.32 (q, *J* = 5.0 Hz, 4H), 4.26 (m, 1H), 4.19 (m, 2H), 3.47 (s, 4H), 2.93 (t, *J* = 5.0 Hz, 1H), 2.37 (m, 1H), 2.32 (m, 4H), 2.13 (s, 12H), 1.79 (m, 4H), 1.52 (m, 4H), 1.22 (m, 4H), 0.98 (t, *J* = 10.0 Hz, 4H). <sup>13</sup>C NMR (125 MHz, DMSO-*d*<sub>6</sub>): δ 172.6, 172.4, 156.8, 153.9, 151.1, 143.7, 143.7, 135.1, 123.5, 116.8, 82.6, 81.5, 74.4, 63.5, 53.7, 49.0, 44.6, 35.6, 33.1, 29.4, 25.3, 23.7. IR (ν<sub>max</sub>): 3322, 3130, 2931, 2859, 2091, 1734, 1687, 1626, 1573, 1165, 1086, 644 cm<sup>-1</sup>. ESI-MS *m/z* 712.70 [M+H]<sup>+</sup>. (**Figure S9-13**)



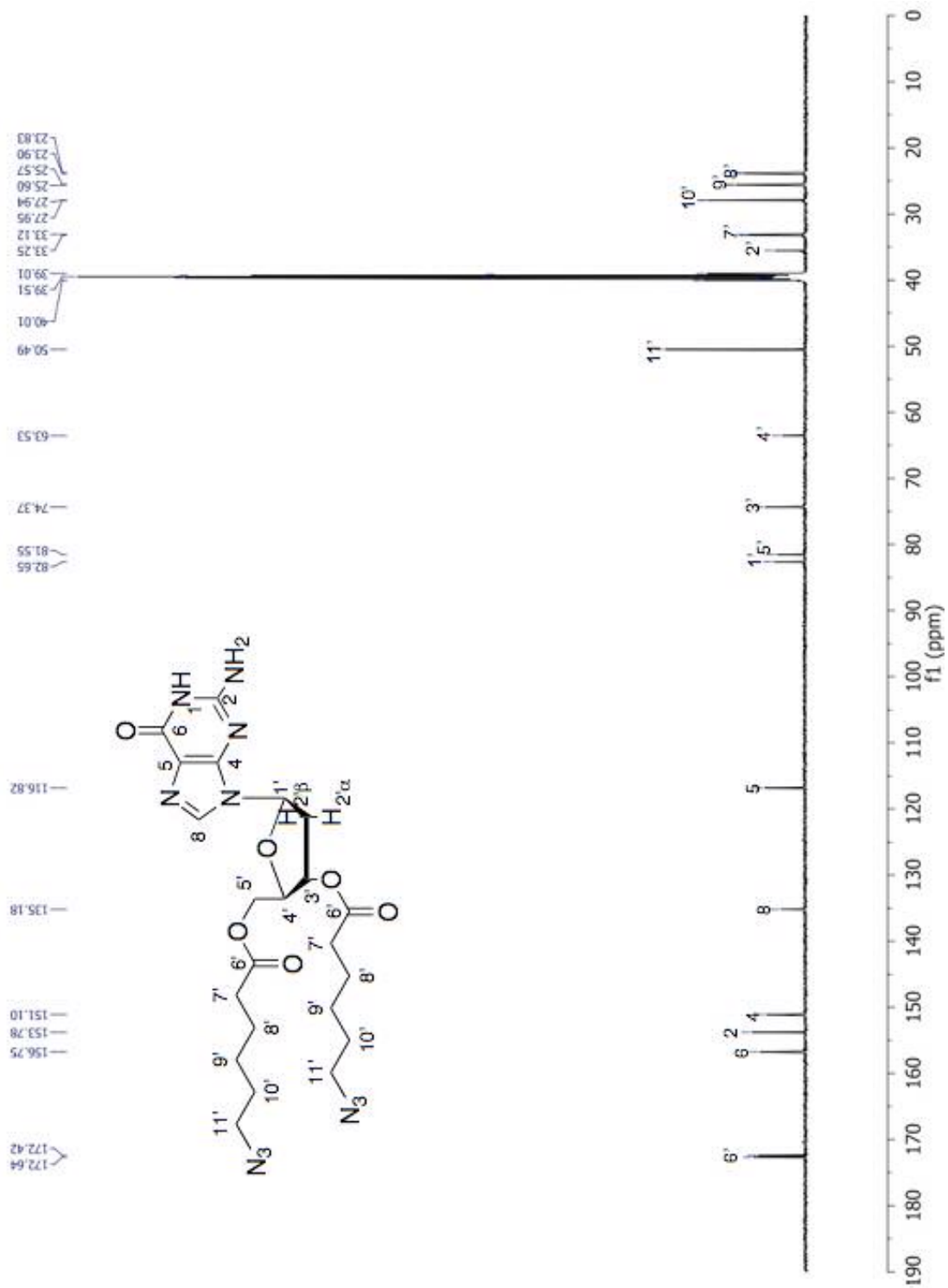


Figure S2.  $^{13}\text{C}$ -NMR (125 MHz) of dGhaz (10 mM) in DMSO- $d_6$ .



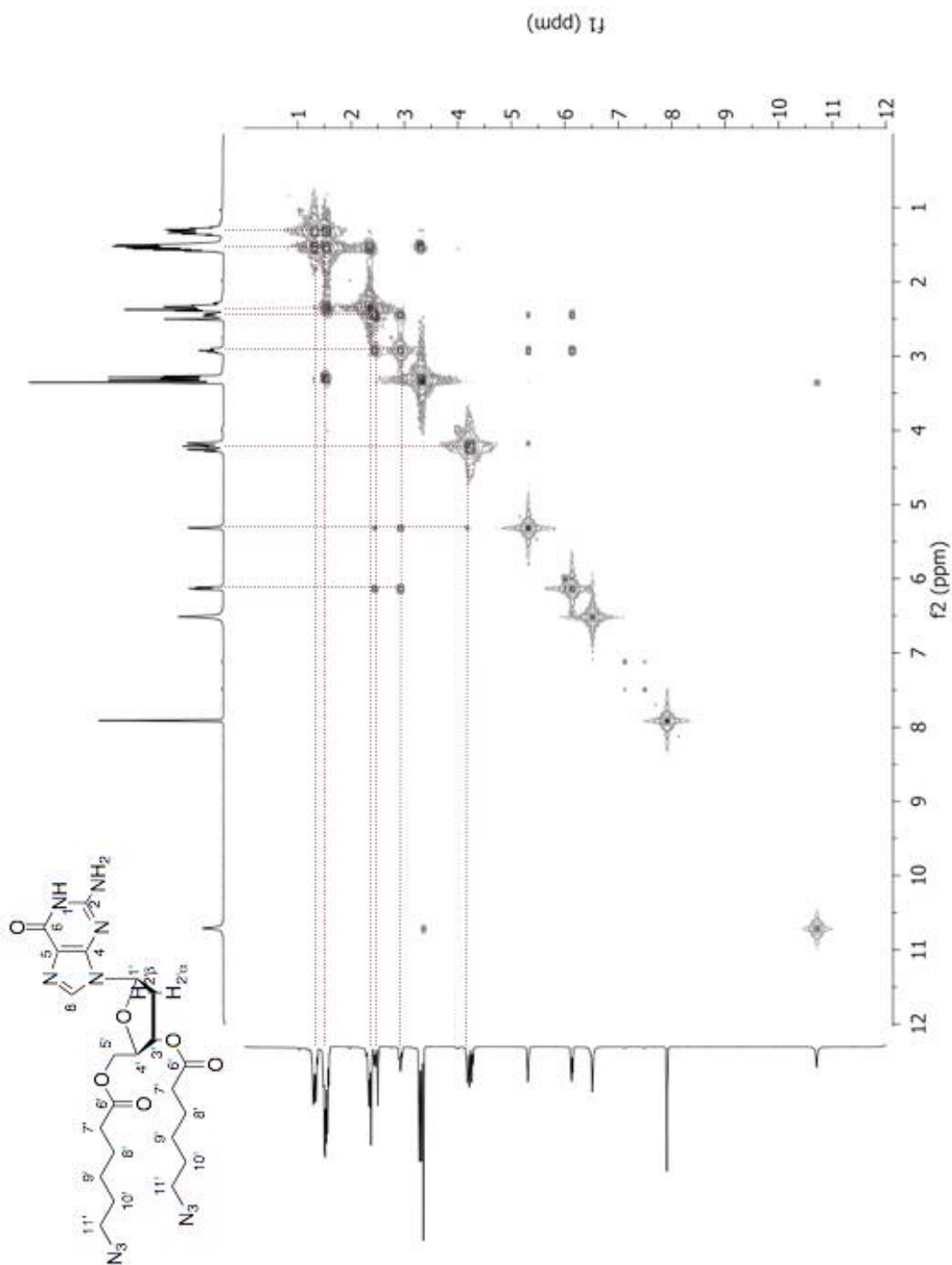


Figure S3. COSY of dGhaz (10 mM) in DMSO-*d*<sub>6</sub>.

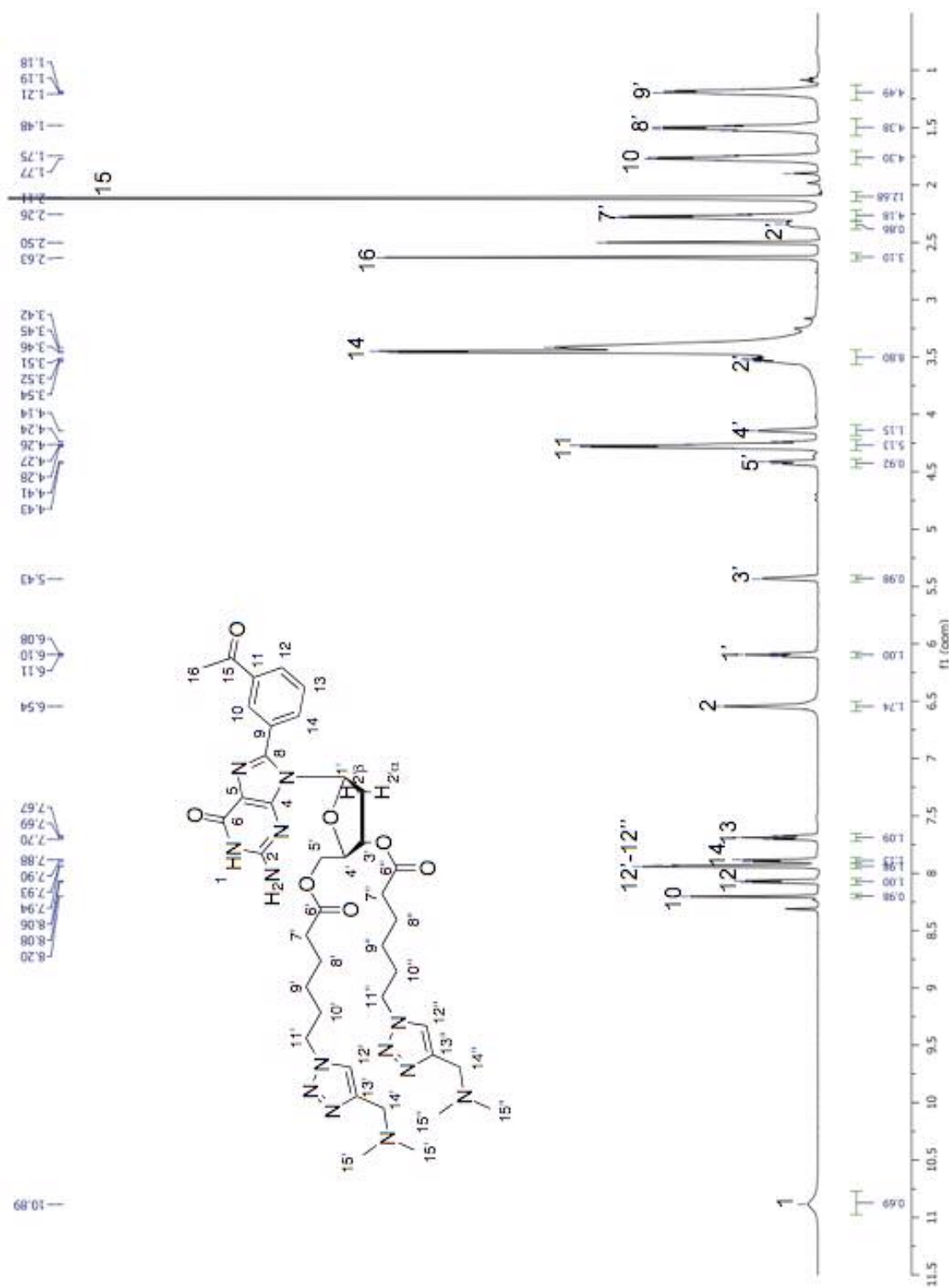


Figure S4.  $^1\text{H-NMR}$  of mAGcat (8 mM) in  $\text{DMSO-}d_6$ .

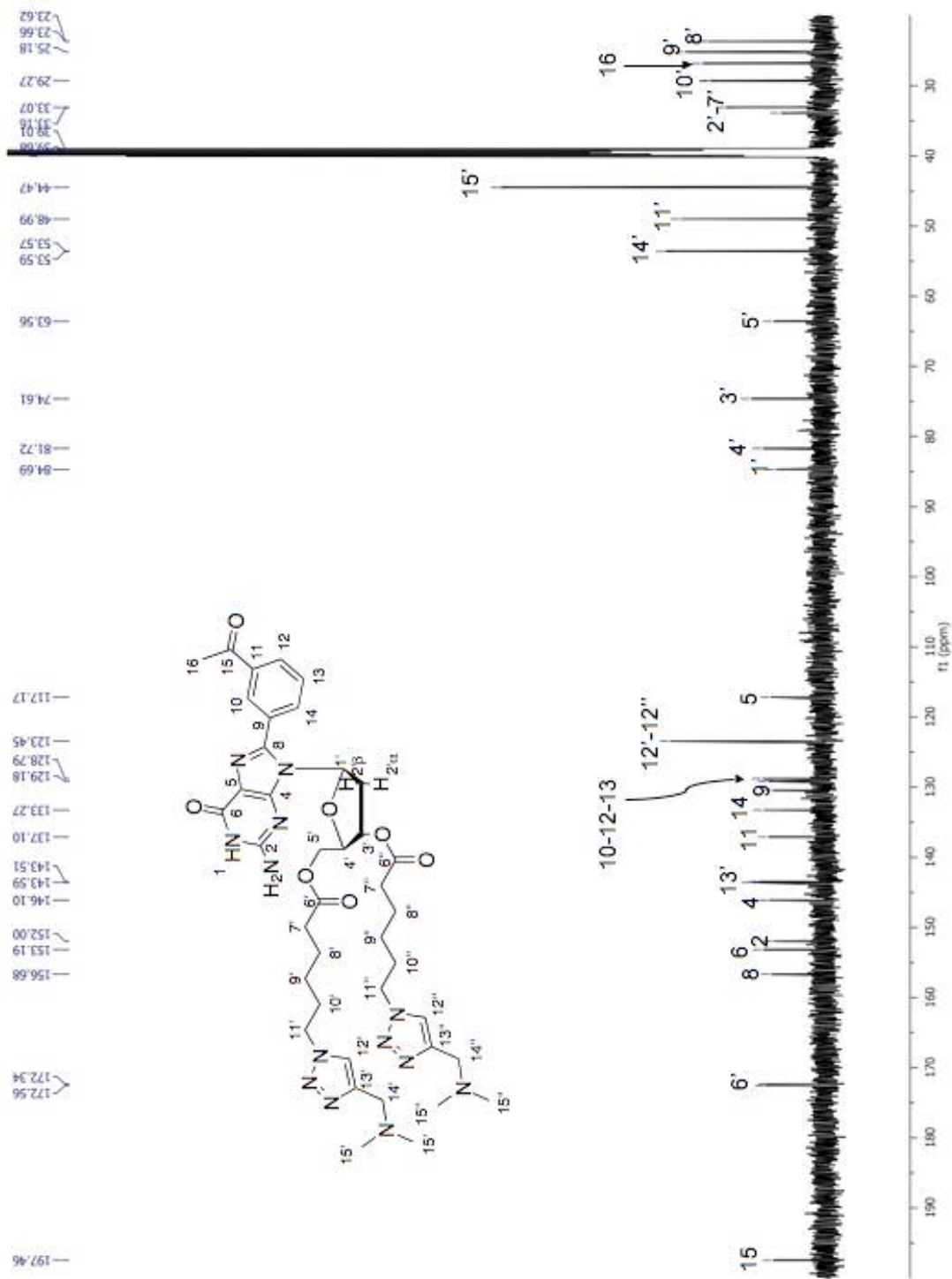


Figure S5.  $^{13}\text{C}$ -NMR (125 MHz) of mAGcat (8 mM) in  $\text{DMSO-}d_6$ .

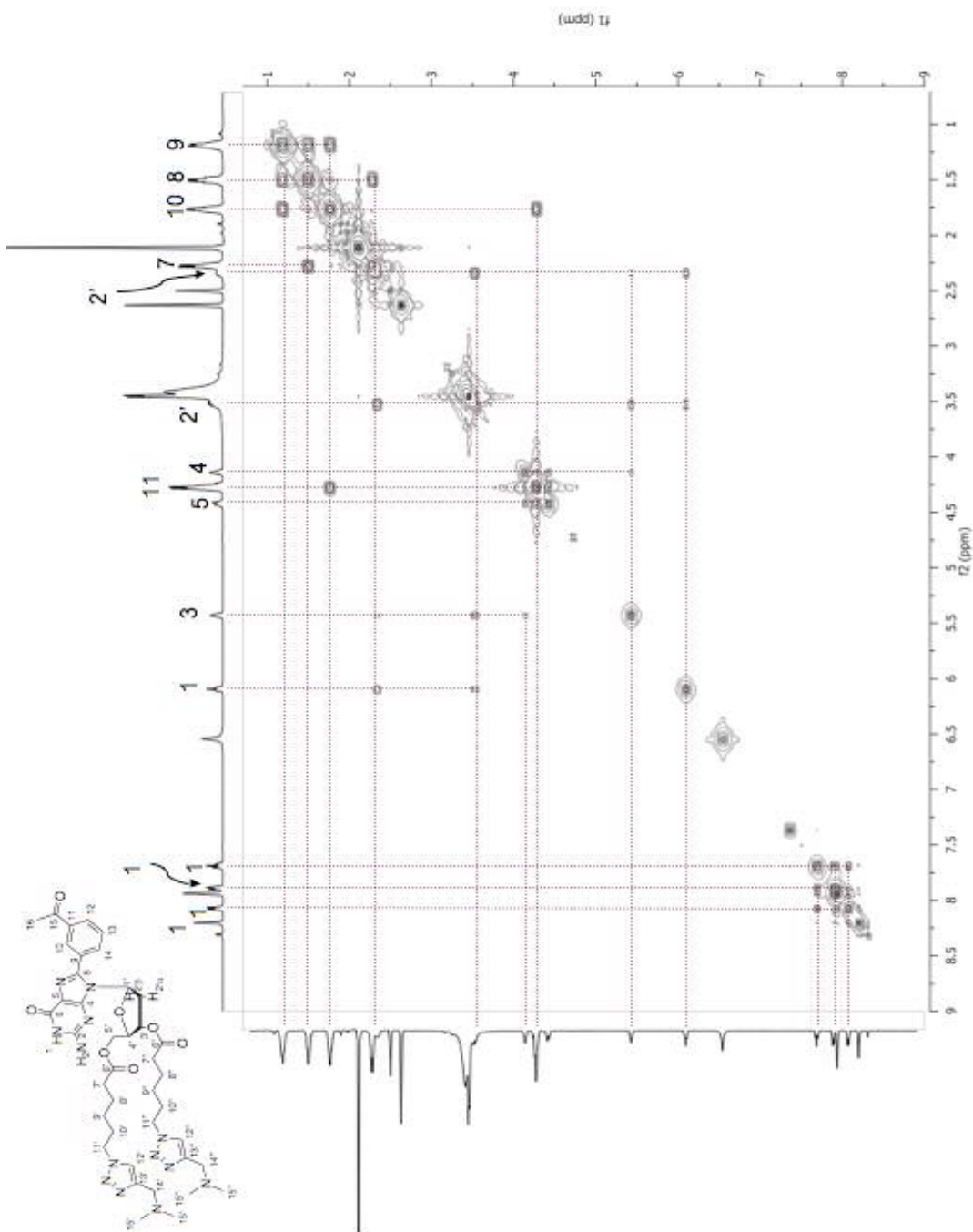
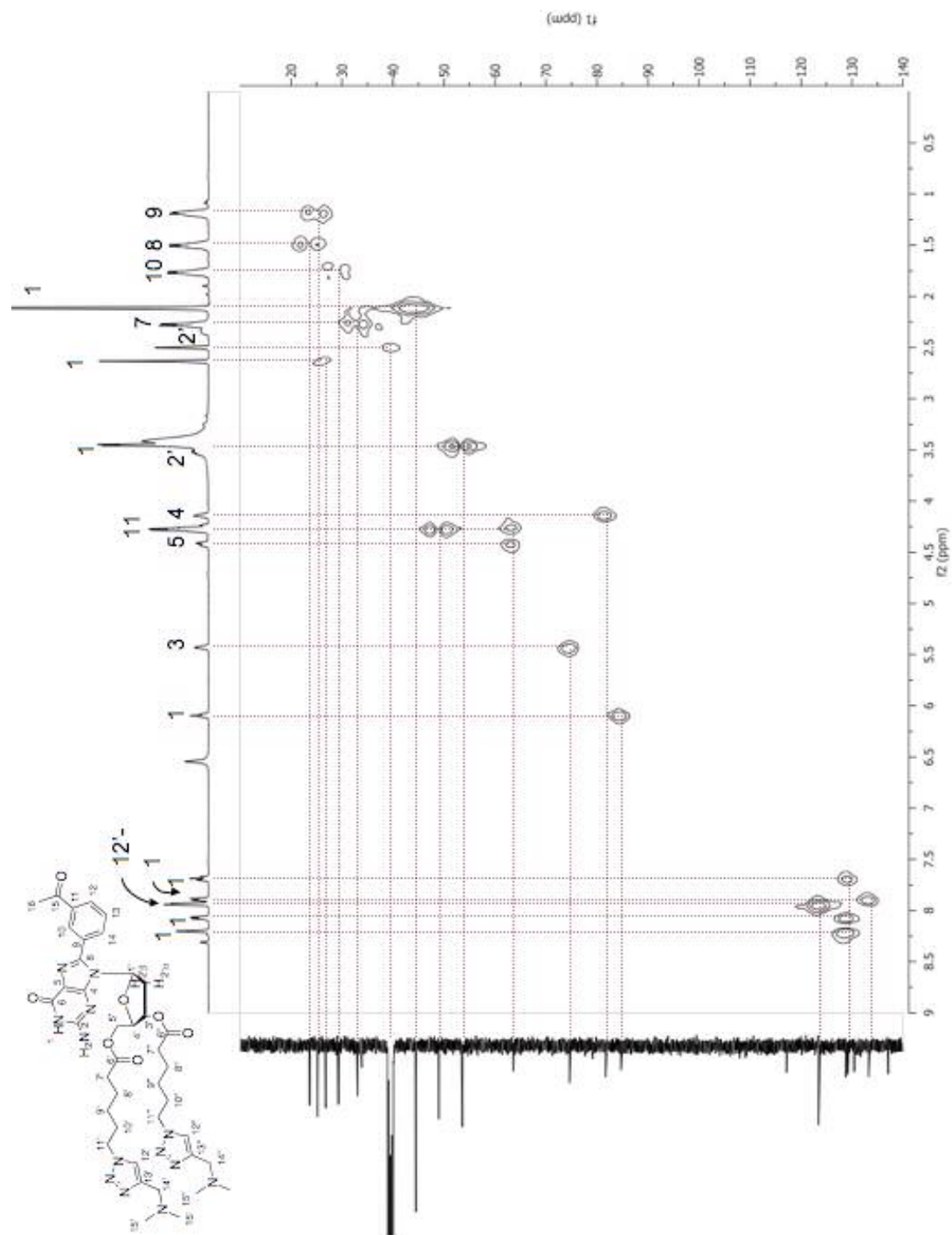
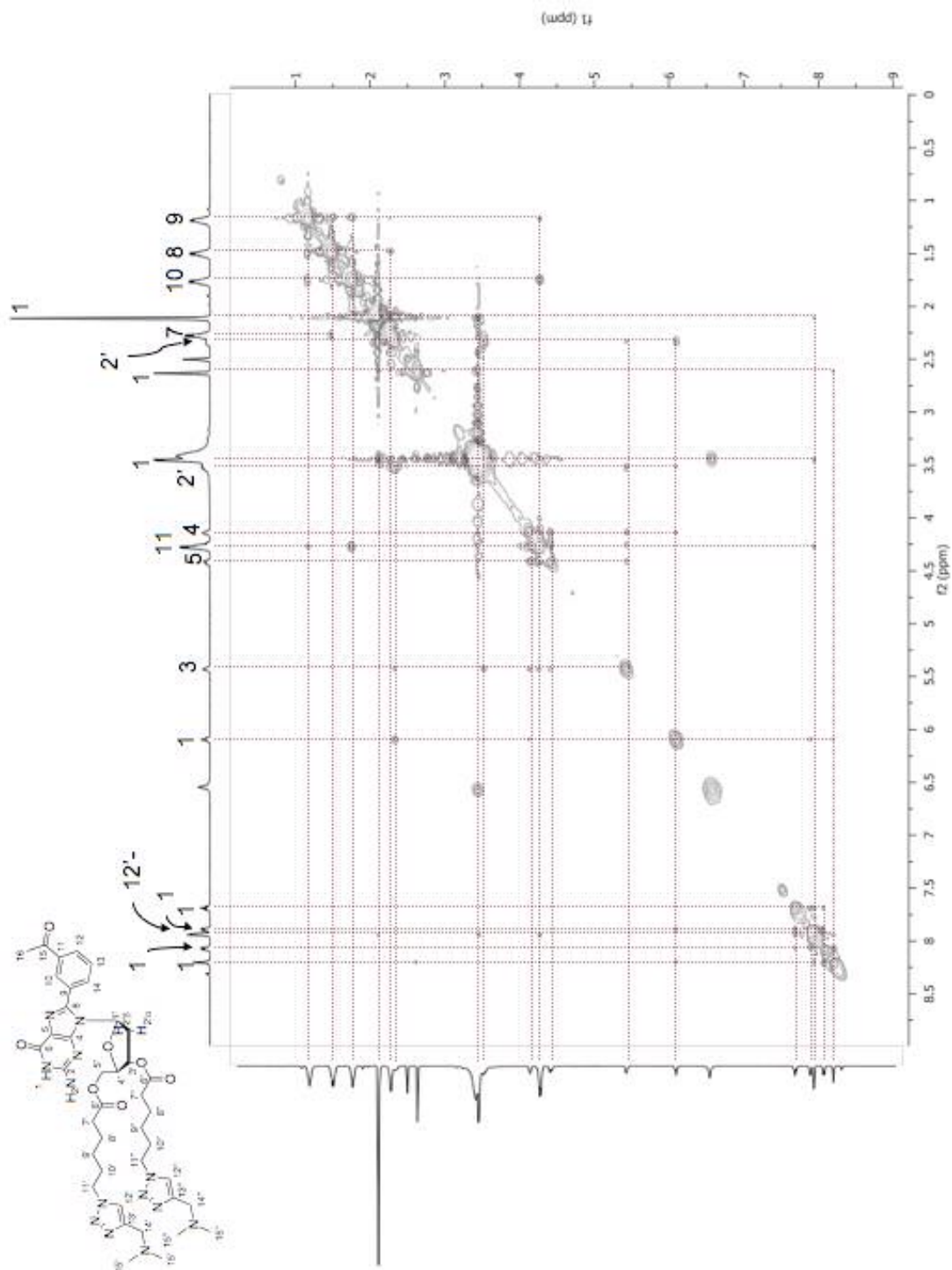


Figure S6. COSY of mAGcat (8 mM) in DMSO-d<sub>6</sub>.





**Figure S8.** NOESY of mAGcat (8 mM) in DMSO-*d*<sub>6</sub> (mixing time 550 ms).

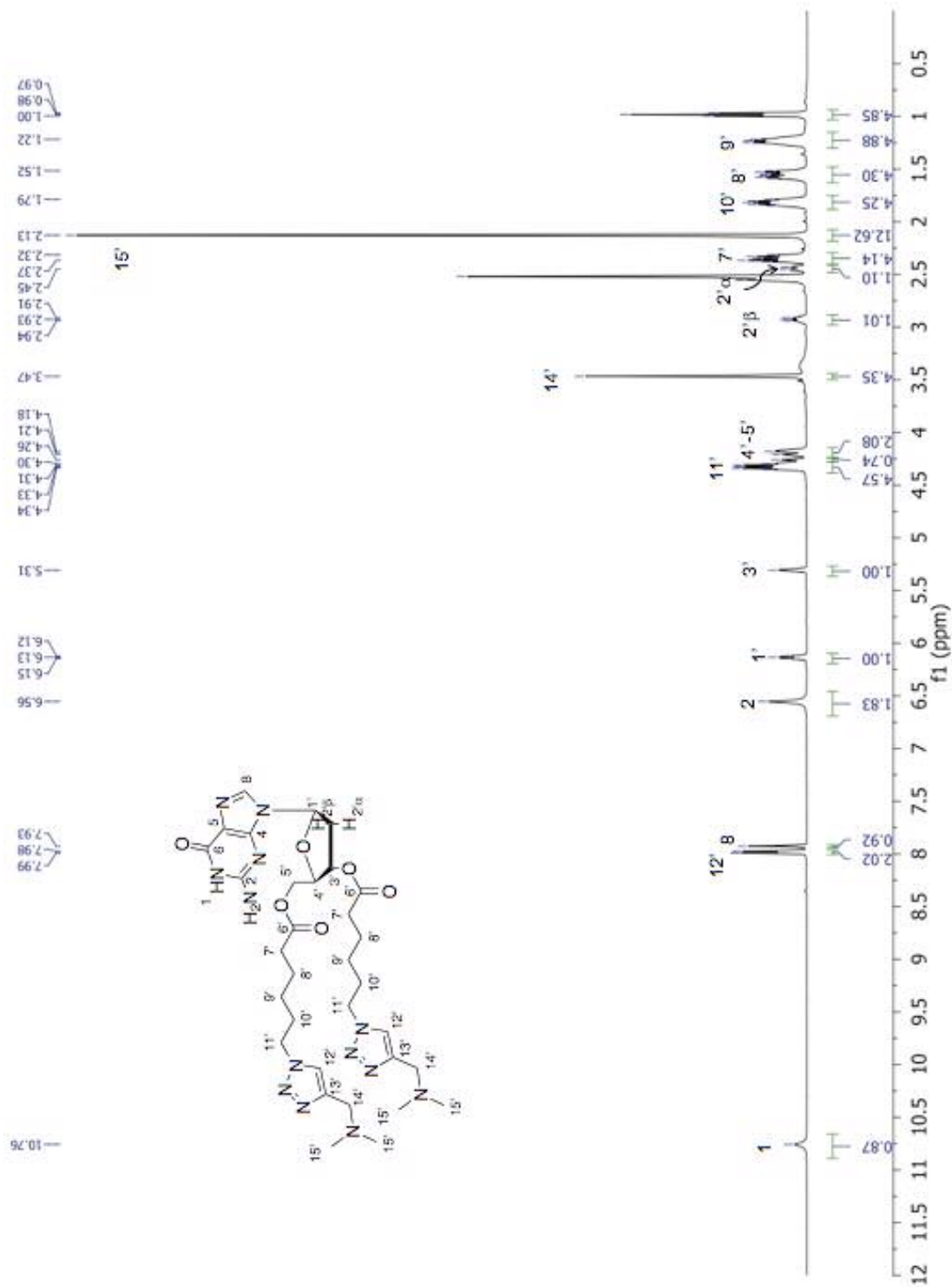
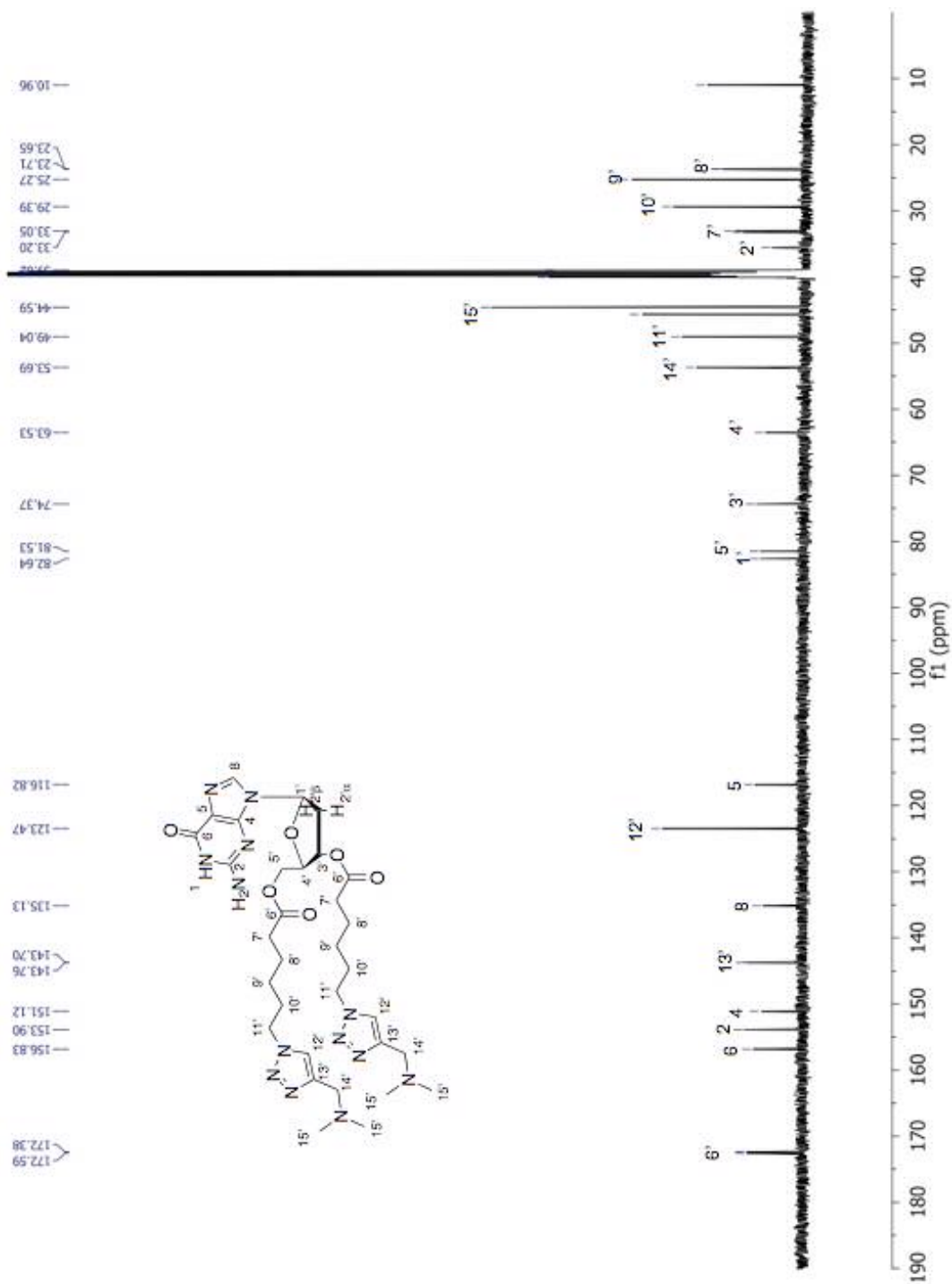
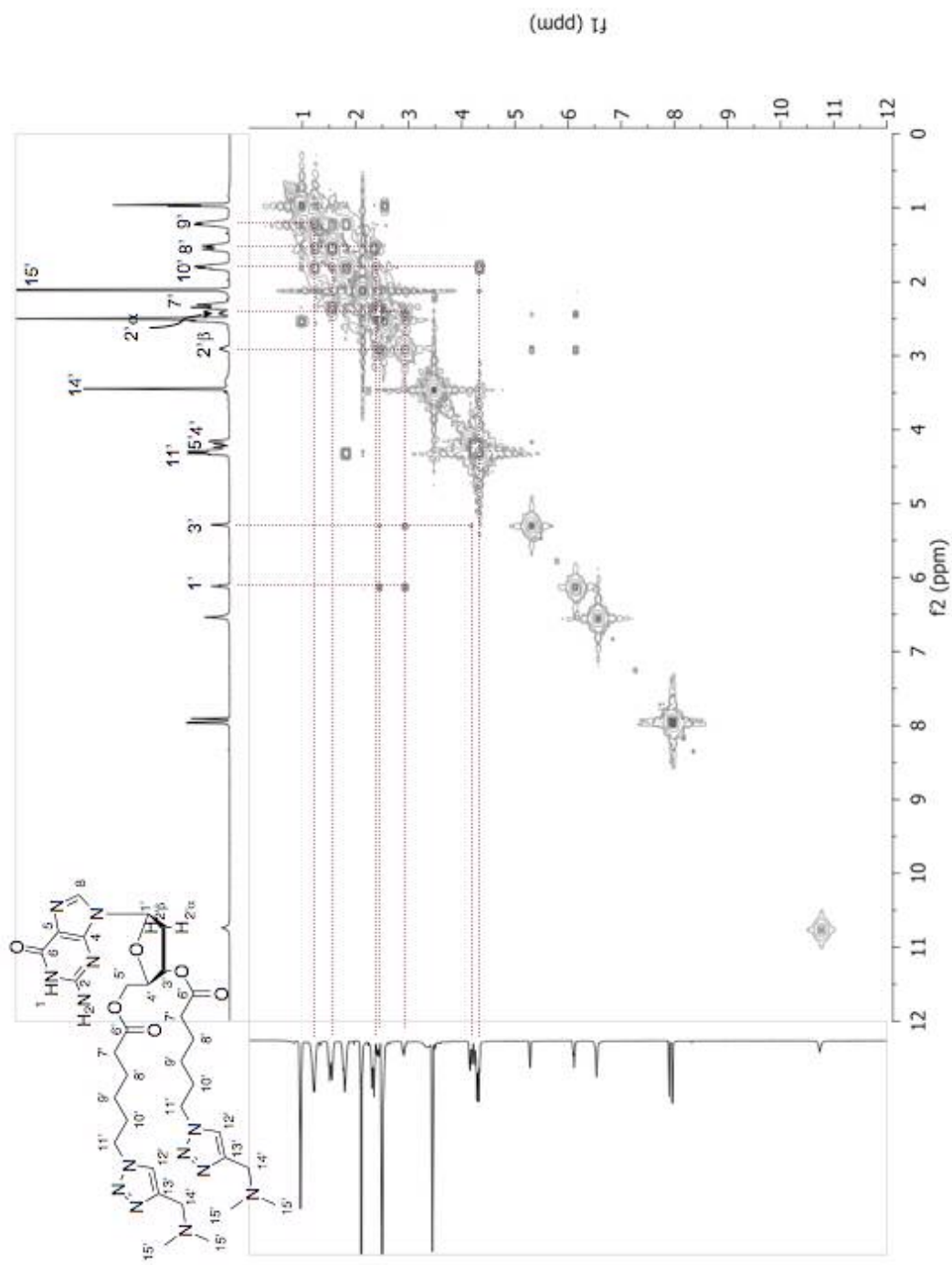


Figure S9.  $^1\text{H-NMR}$  of dGcat (8 mM) in  $\text{DMSO-}d_6$ .



**Figure S10.**  $^{13}\text{C}$ -NMR (125 MHz) of dGcat (8 mM) in  $\text{DMSO-}d_6$ .





**Figure S11.** COSY of **dGcat** (8 mM) in DMSO-*d*<sub>6</sub>.

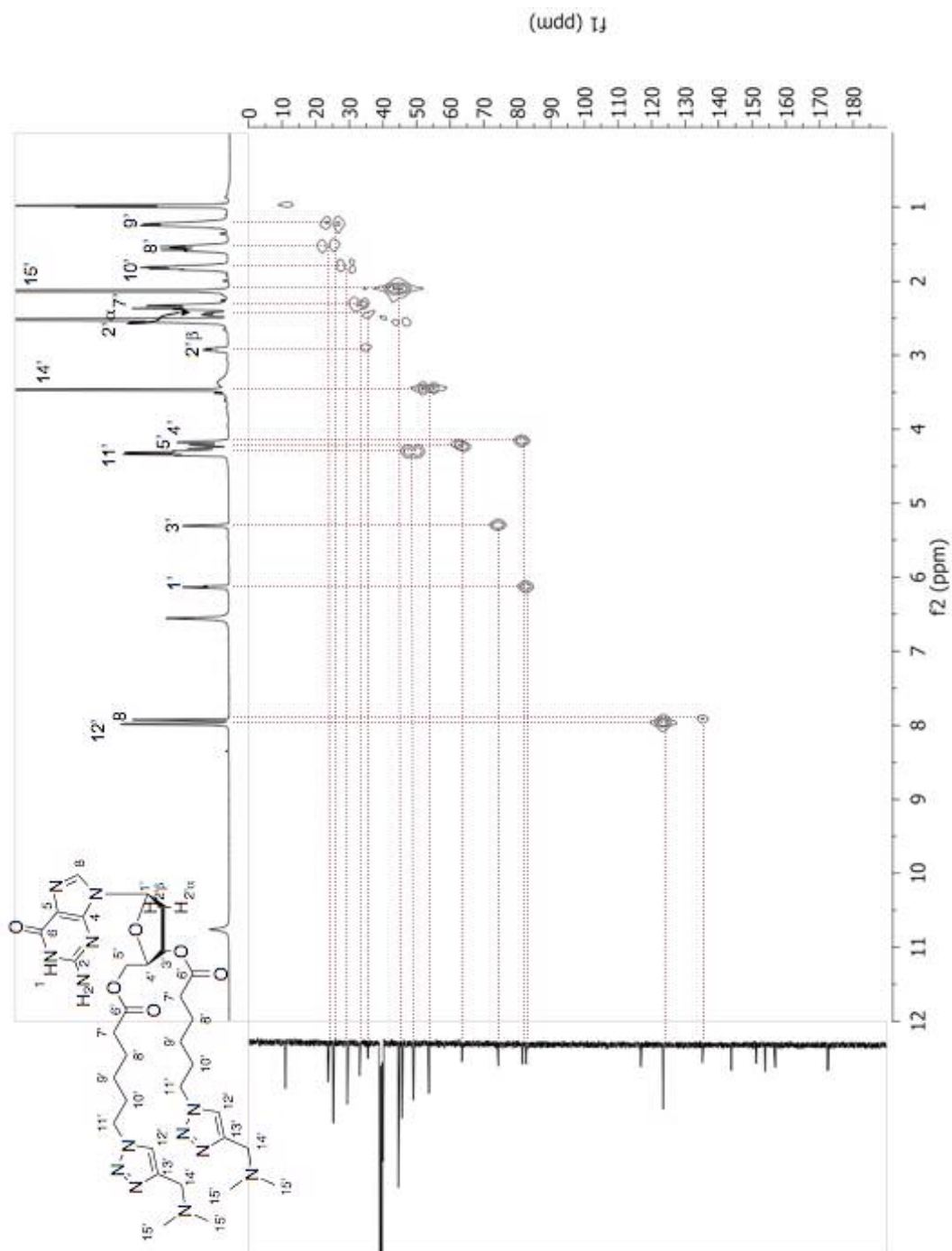
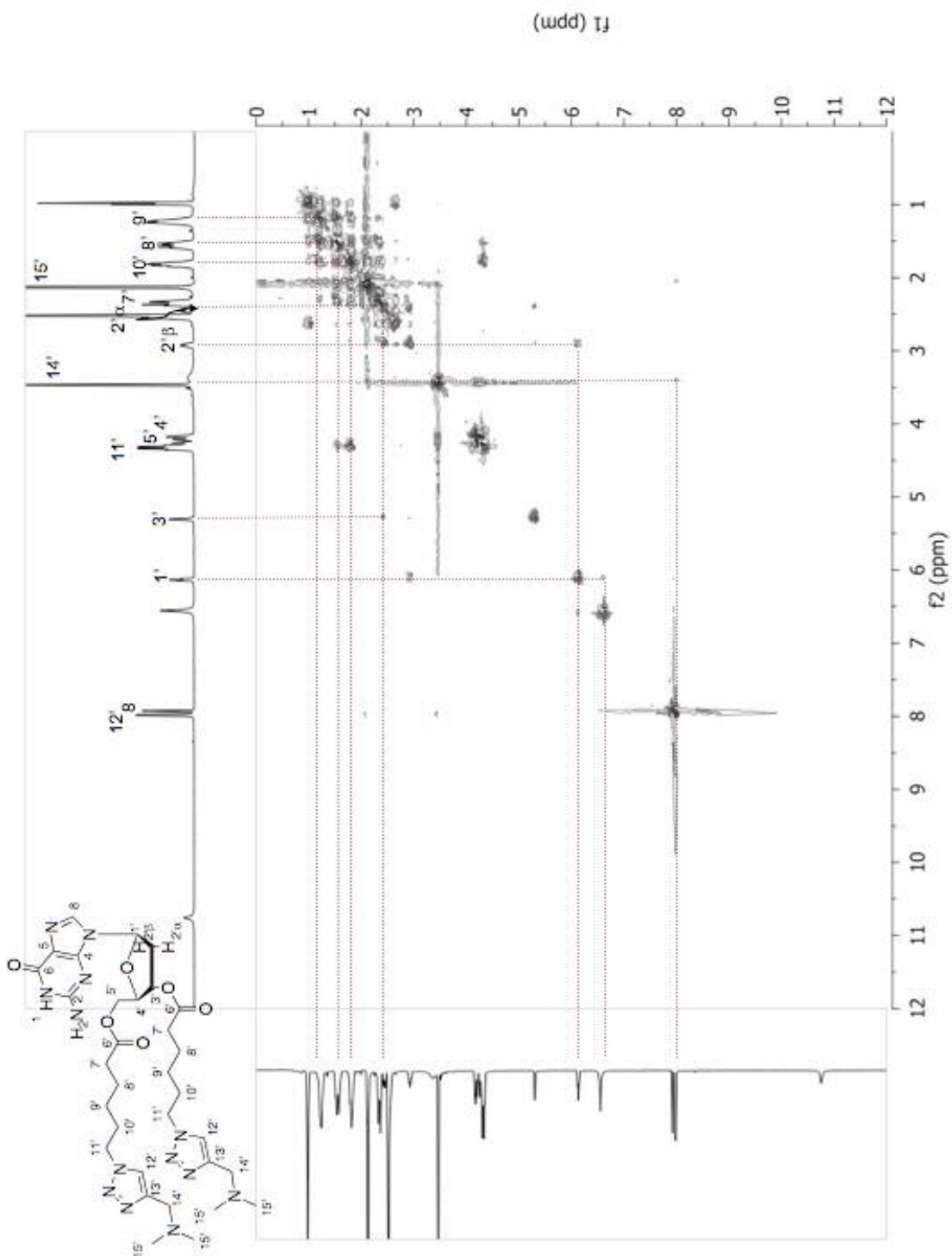
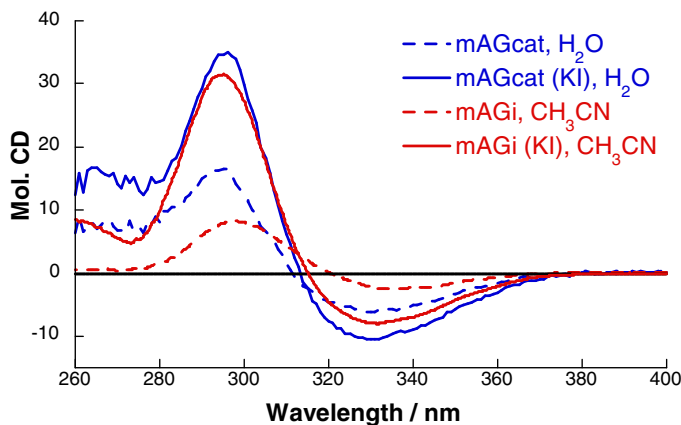


Figure S12. HMBC of dGcat (8 mM) in DMSO-*d*<sub>6</sub>.



**Figure S13.** NOESY of dGcat (8 mM) in DMSO-*d*<sub>6</sub> (mixing time 200 ms).

## Circular Dichroism (CD) Spectroscopy



**Figure S14.** CD spectra of **mAGi** (10 mM) and **mAGcat** (5 mM), with and without KI.

CD spectroscopy studies were carried out in CH<sub>3</sub>CN and H<sub>2</sub>O, at 20°C, in the 400-200 nm wavelength region at 0.2 nm resolution using a 1.0 cm quartz cell. The solvent reference spectrum was used as baseline and digitally subtracted from the CD spectra.

### *Self-assembly studies*

Self-assembly studies were carried out using a Bruker DRX-500 NMR spectrometer, equipped with either a 5 mm BBO or a TXI probe. In water, a conventional 1D presaturation pulse sequence with the excitation pulse set over the water peak at 4.7 ppm was used. A standard proton sequence was used for experiments in D<sub>2</sub>O. Self-assembly studies were performed, for example, using a 10 mM solution of **mAGcat** in 600 μL of H<sub>2</sub>O-D<sub>2</sub>O (9:1) or D<sub>2</sub>O. For the NOESY experiment a phase-sensitive 2D NOESY pulse sequence with presaturation (noesyphpr) was used. For NOESY and COSY in D<sub>2</sub>O standard pulse sequences were used.

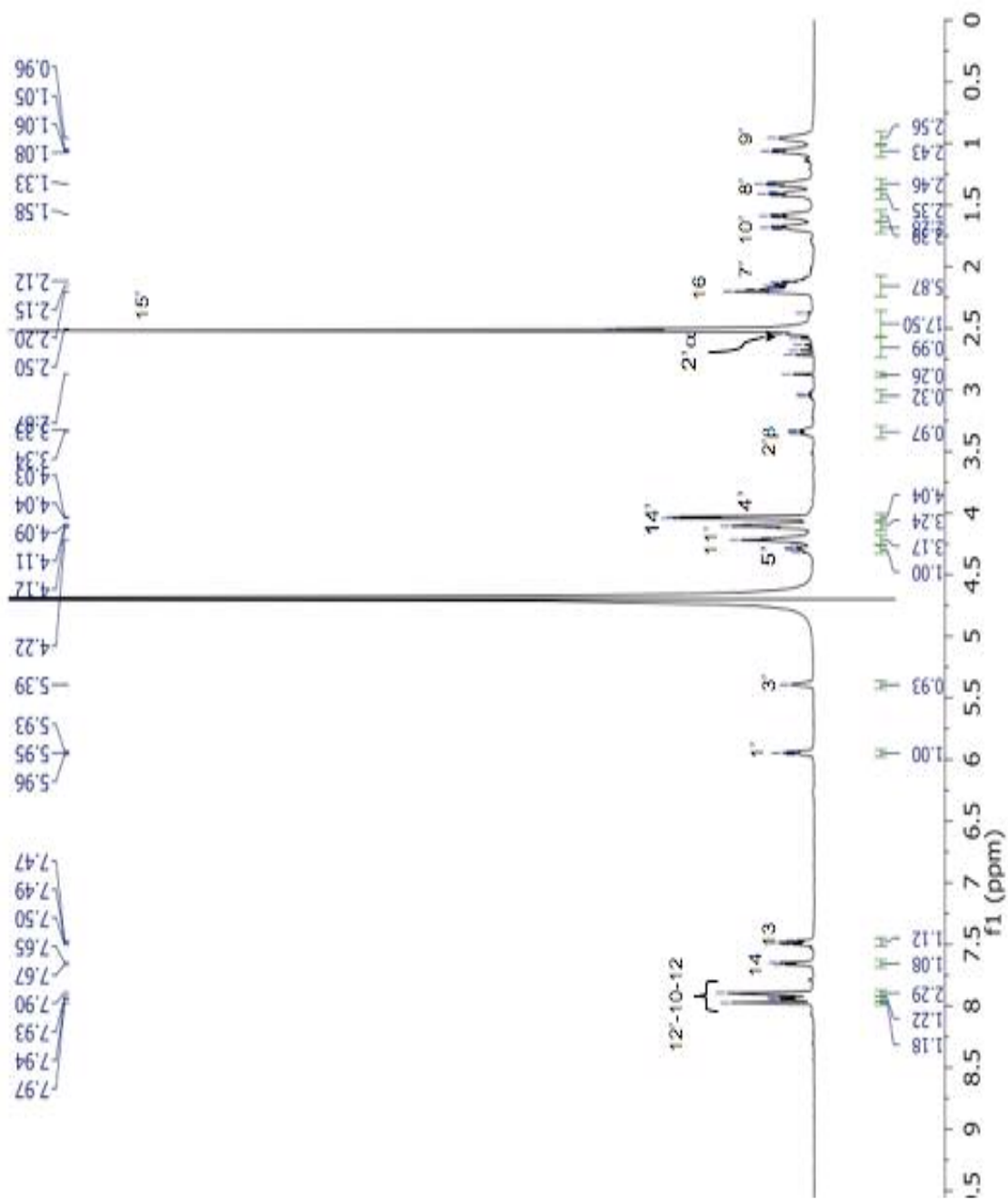


**Figure S15.**  $^1\text{H-NMR}$  of mAGcat (10 mM) in  $\text{H}_2\text{O-D}_2\text{O}$  (9:1).

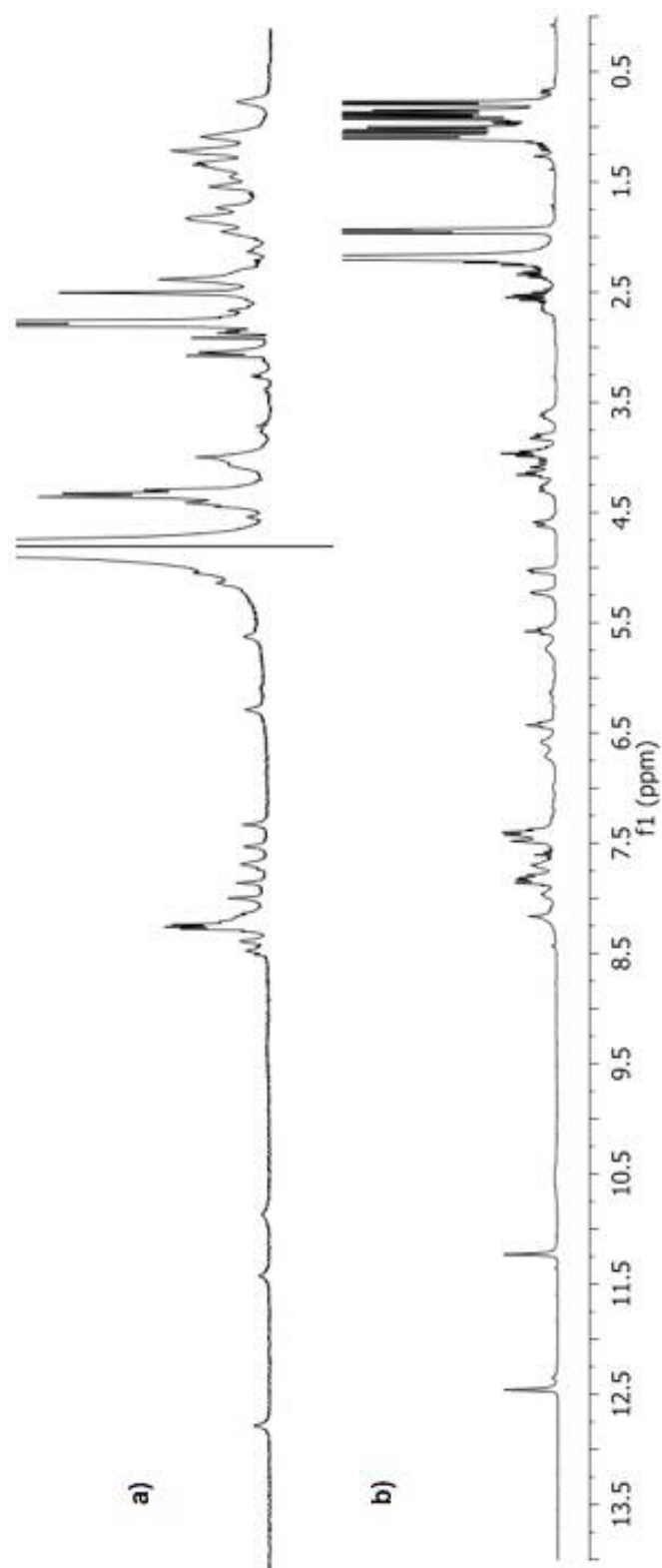


**Figure S16.** <sup>1</sup>H-NMR of: a) **mAGcat** (10 mM) with KCl (1 M) in H<sub>2</sub>O-D<sub>2</sub>O (9:1) and b) **mAGi** (50 mM) with KI (25 mM) in CD<sub>3</sub>CN.

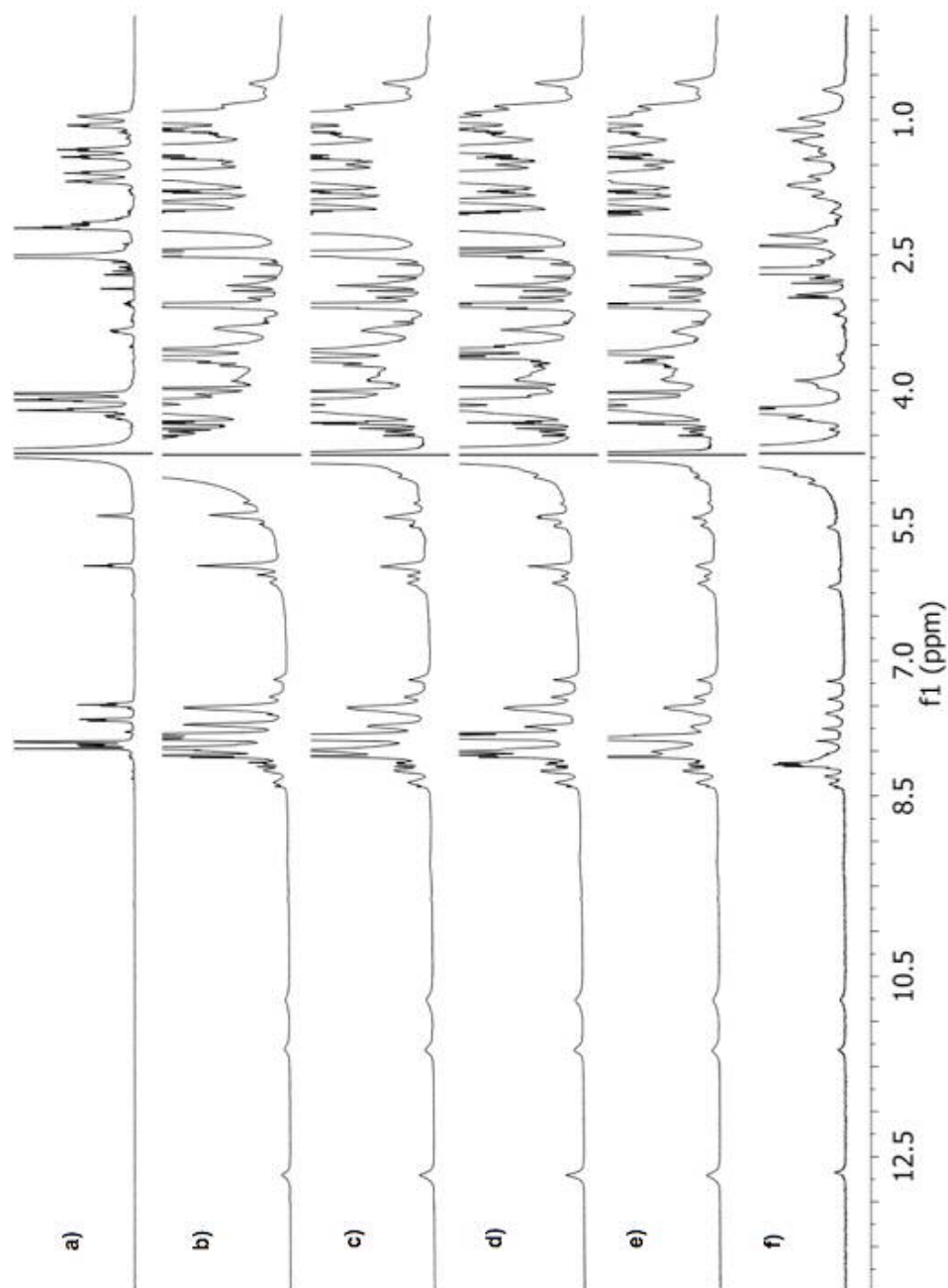


**Figure S17.**  $^1\text{H}$ -NMR titration of **mAGcat** (10 mM) in  $\text{H}_2\text{O}$ - $\text{D}_2\text{O}$  (9:1) with increasing amounts of KCl. a) with no KCl, no detectable amount of hexadecamer (Hx), b) 0.63 mM KCl, 31 % Hx, c) 1.25 mM KCl, 50 % Hx, d) 2.00 mM KCl, 51 % Hx, e) 5.00 mM KCl, 60 % Hx, and f) 1 M KCl, 92 % Hx.

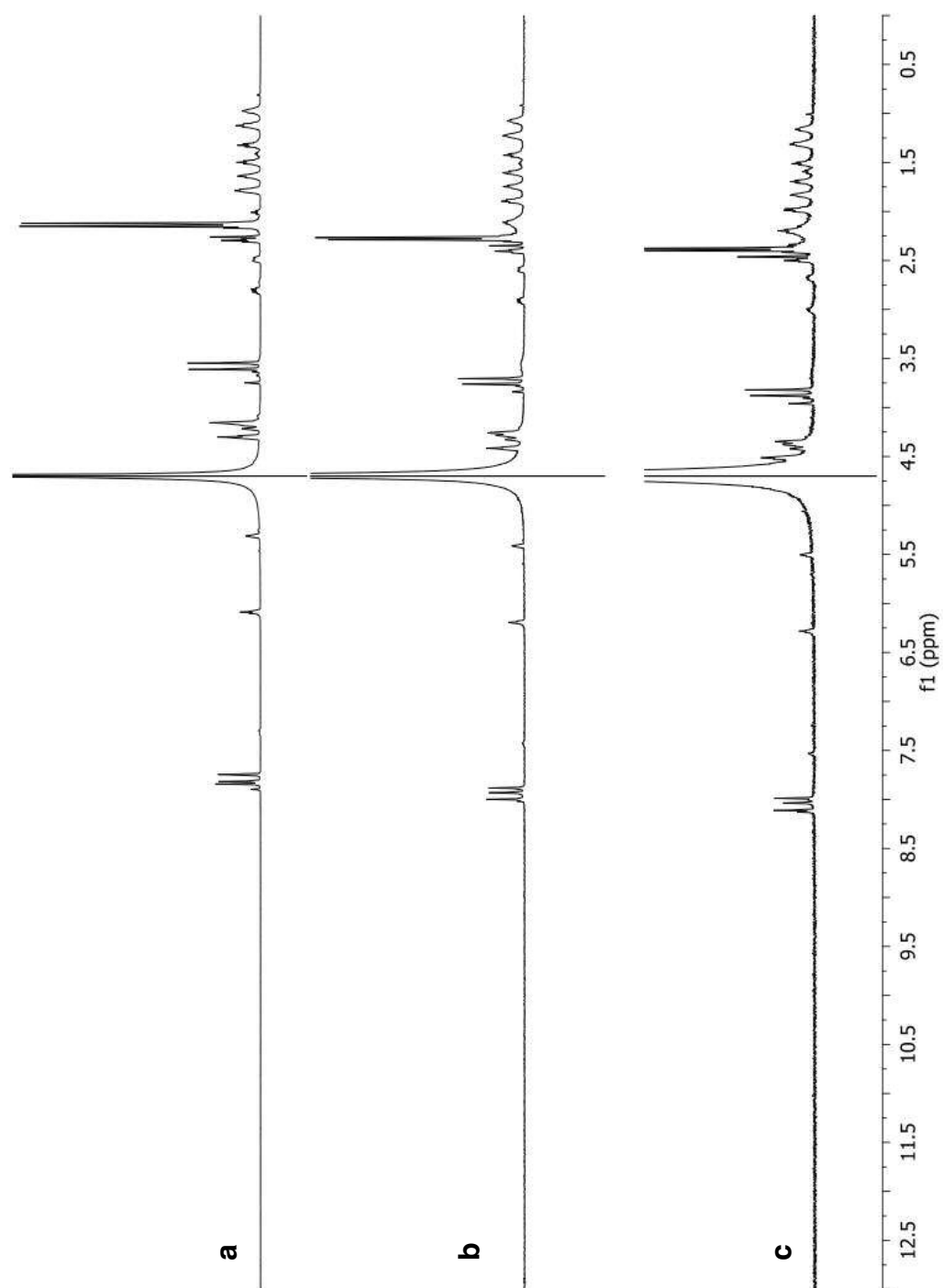


**Figure S18.** <sup>1</sup>H-NMR of a) **dGcat** (10 mM), with no KCl in H<sub>2</sub>O-D<sub>2</sub>O (9:1); b) **dGcat** (10 mM), 1 M KCl in H<sub>2</sub>O-D<sub>2</sub>O (9:1); and c) **dGcat** (10 mM), 2 M KCl in H<sub>2</sub>O-D<sub>2</sub>O (9:1).



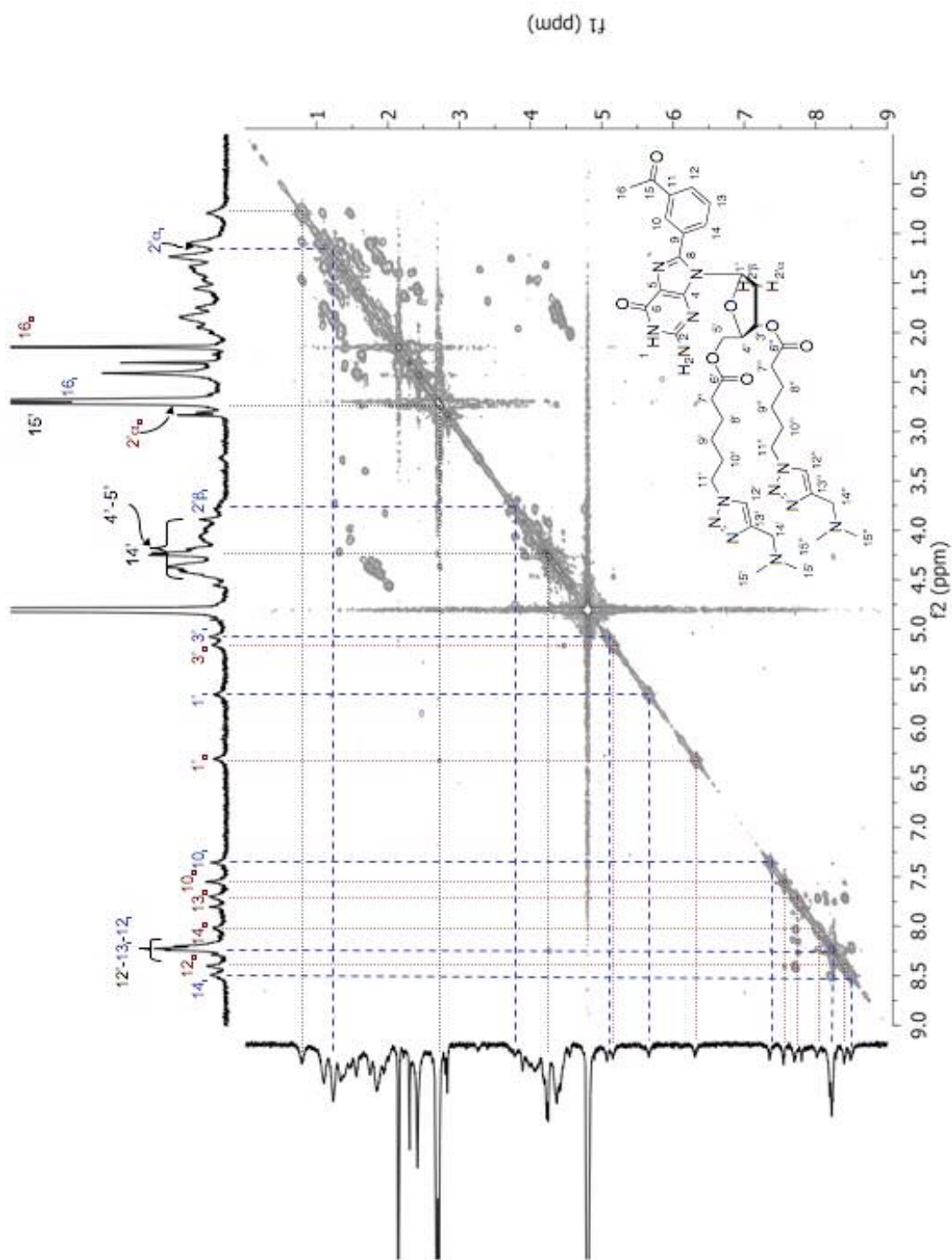


Figure S19. COSY of mAGcat (10 mM) 1M KCl in D<sub>2</sub>O.

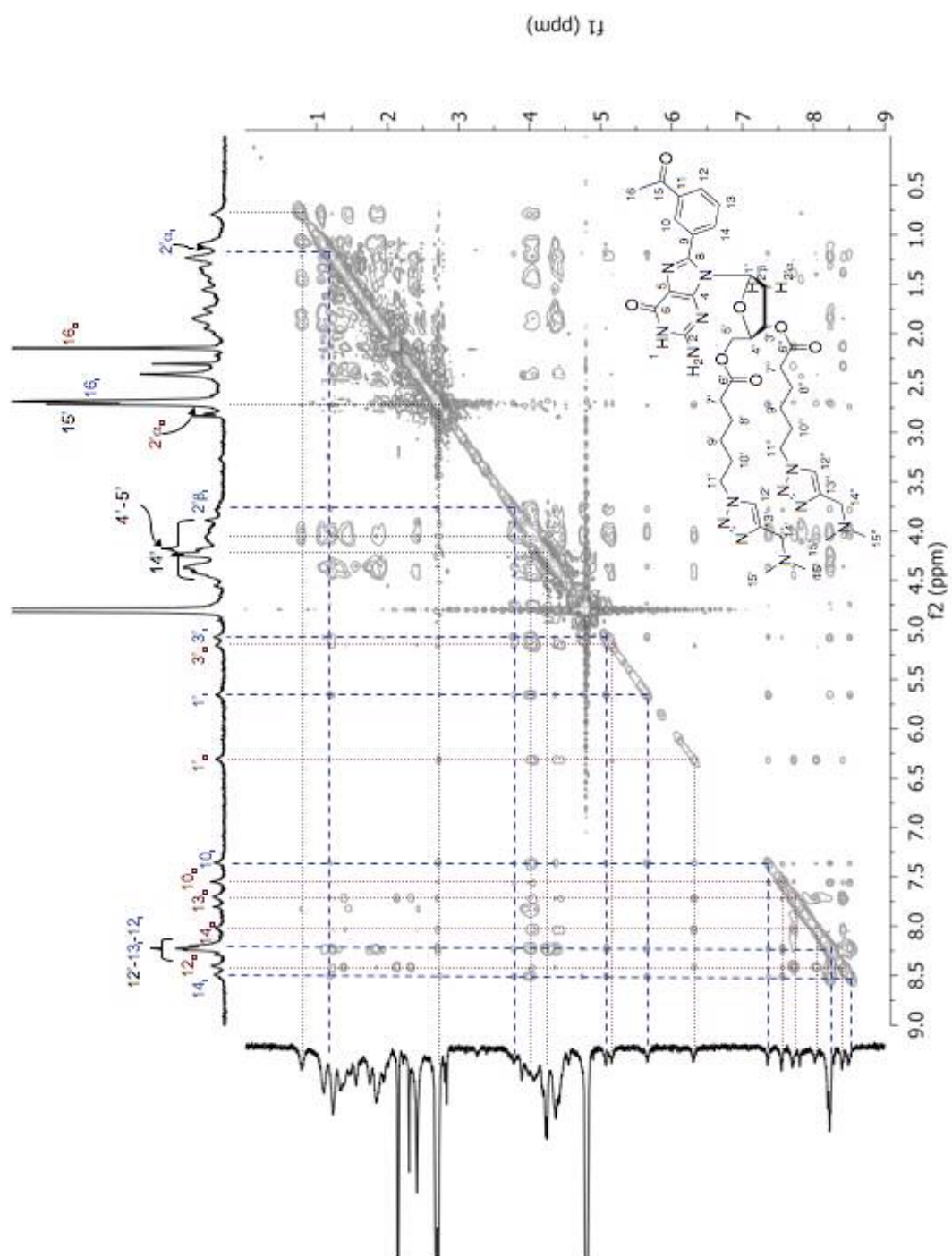
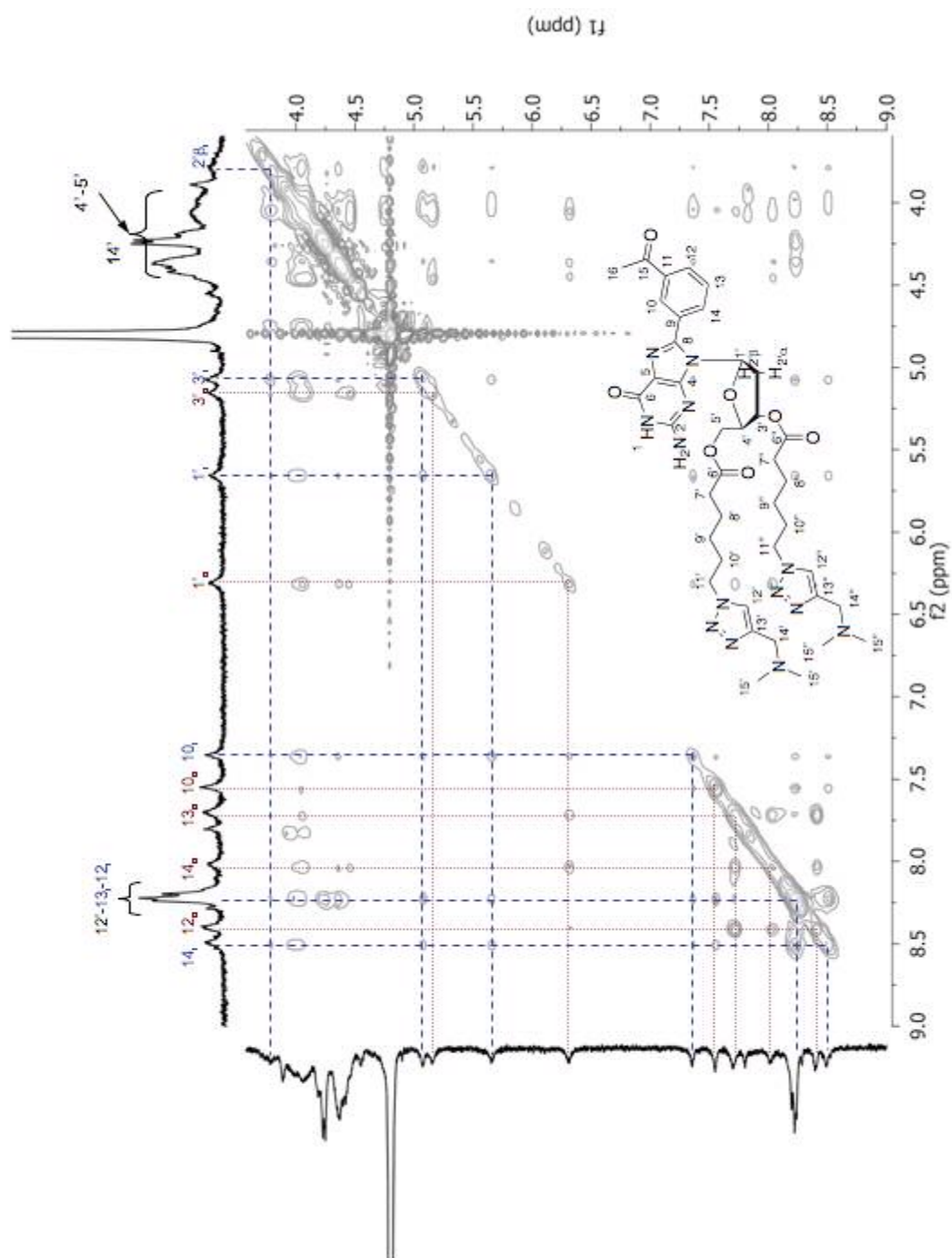


Figure S20. NOESY of mAGcat (10 mM) 1M KCl in D<sub>2</sub>O (mixing time 500 ms).



**Figure S21.** Expansion of the NOESY of **mAGcat** (10 mM) 1M KCl in D<sub>2</sub>O (mixing time 500 ms).

QuickTime™ and a  
decompressor  
are needed to see this picture.

**Figure S22.** NOESY of **mAGcat** (10 mM) 1M KCl in H<sub>2</sub>O-D<sub>2</sub>O (9:1) (mixing time 410 ms).

**Figure S23.** Expansion of the NOESY of **mAGcat** (10 mM) 1 M KCl in H<sub>2</sub>O-D<sub>2</sub>O (9:1) (mixing

QuickTime™ and a  
decompressor  
are needed to see this picture.

time 410 ms).

This section of the NOESY, which corresponds to figure 2 in the main text, shows the connectivities between the subunits in the outer tetrad and the subunits in the inner tetrad.

As such those NOEs can only arise from an assembled hexadecamer as described in the main text. The connectivities are  $\text{NH}_2^{\text{H}}_{\text{o}}\text{-NH}_2^{\text{wc}}_{\text{o}}$ ,  $\text{NH}_2^{\text{wc}}_{\text{o}}/\text{NH}_2^{\text{H}}_{\text{o}}\text{-NH1}_{\text{o}}$ ,  $\text{NH}_2^{\text{wc}}_{\text{i}}/\text{NH}_2^{\text{wc}}_{\text{o}}$ ,  $\text{NH}_2^{\text{wc}}_{\text{o}}/\text{NH}_2^{\text{H}}_{\text{o}}\text{-H10}_{\text{i}}$  and  $\text{NH1}_{\text{i}}/\text{NH}_2^{\text{wc}}_{\text{i}}\text{-NH1}_{\text{o}}$ .

QuickTime™ and a  
decompressor  
are needed to see this picture.

QuickTime™ and a  
decompressor  
are needed to see this picture.

**Figure S24.** Detailed explanation of the connectivities shown in Figure 2a from the main text.

### ***Diffusion NMR studies***

Pulsed field gradient diffusion experiments were carried out with a Bruker DRX-500, equipped with a 5 mm BBO probe, spectrometer using the Stimulated Echo Pulse Gradient sequence (stebpgpls) in FT mode. To improve homogeneity a “13 interval pulse sequence” was used with two pairs of bipolar gradients. The shape of the gradient used was sine and the temperature was actively controlled at  $25.0 \pm 0.5$  °C. Diffusion coefficients were derived using integration of the desired peaks to a single exponential decay, using the Bruker software package T1/T2 Relaxation (TopSpin v 2.0). Calculation of the hydrodynamic radius in D<sub>2</sub>O used the viscosity value ( $\eta = 1.103$  Kg m<sup>-1</sup> s<sup>-1</sup>, 298.15 °K) reported in the literature.<sup>1</sup> The hydrodynamic radii of the species in the NMR tube were calculated according to the spherical approximation using the Einstein-Stokes equation:

$$D = \frac{k_B T}{6\pi\eta r_H}$$

where  $T$  denotes the temperature,  $\eta$  is the viscosity of the solvent at the given temperature,  $k_B$  is the Boltzmann-Constant,  $D$  is measured diffusion constant and  $r_H$  is the hydrodynamic radius. The data were further processed by the Bruker software package.

---

<sup>1</sup> *One of the largest effects of dissolved salts in the diffusion rates of solutes in water relates to changes in the viscosity of the solvent and the value used in the Einstein-Stokes equation. For salts containing cations that interact strongly with water (e.g. Li<sup>+</sup>, Na<sup>+</sup>, Mg<sup>2+</sup>, etc.) there is a significant non-linear increase in the viscosity of the medium, which is particularly pronounced for concentrations above 2 M. In contrast, the viscosity of KCl remains essentially constant from 0-4 M. This phenomenon results from the poorer solvation of the potassium cations when compared to the cations mentioned previously. (For more information see: (a) Kevin L. Gering, *Electrochimica Acta*, 51, 2006, 3125-3138; (b) D. R. Lide, Editor in Chief, *CRC Handbook of Chemistry and Physics*, 79 th Ed., CRC Press, Boca Ranton, Florida, 1998). Therefore, the value used in our calculations was the one for pure D<sub>2</sub>O.*

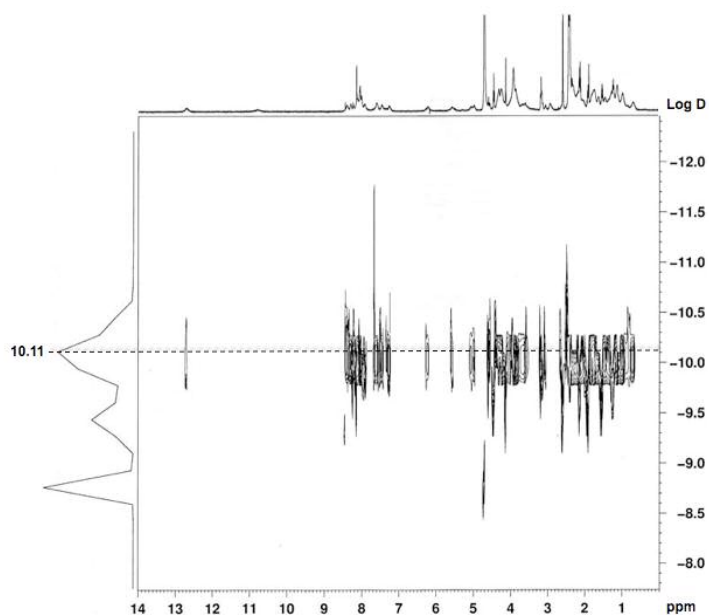


**Figure S25.** DOSY of **mAGcat** (10 mM) 1M KCl in D<sub>2</sub>O.

To corroborate the hydrodynamic radius energy minimizations of **mAGcat** were performed. Computed using AMBER\* (MacroModel, Version 9.5, Maestro 8.0.315, Schrödinger, LLC, New York, NY, 2007) representing water as a continuum solvent. The hydrodynamic radius ( $r'_H$ ) of 25.5 Å is in agreement with that obtained from the diffusion coefficient (D) for a hexadecamer of 24.8 Å (Figure S26). Although, the corresponding values for models of a dodecamer (24.2 Å) or a 20-mer (28.2 Å) are not far off, they can be rejected based on the symmetry reflected in the NMR spectra (O<sub>D4</sub>). A hypothetical octamer (23.9 Å) would be too small and, although it could share the same symmetry, it was rejected based on the 2D-NOESY experiments (Figures S20-S24).



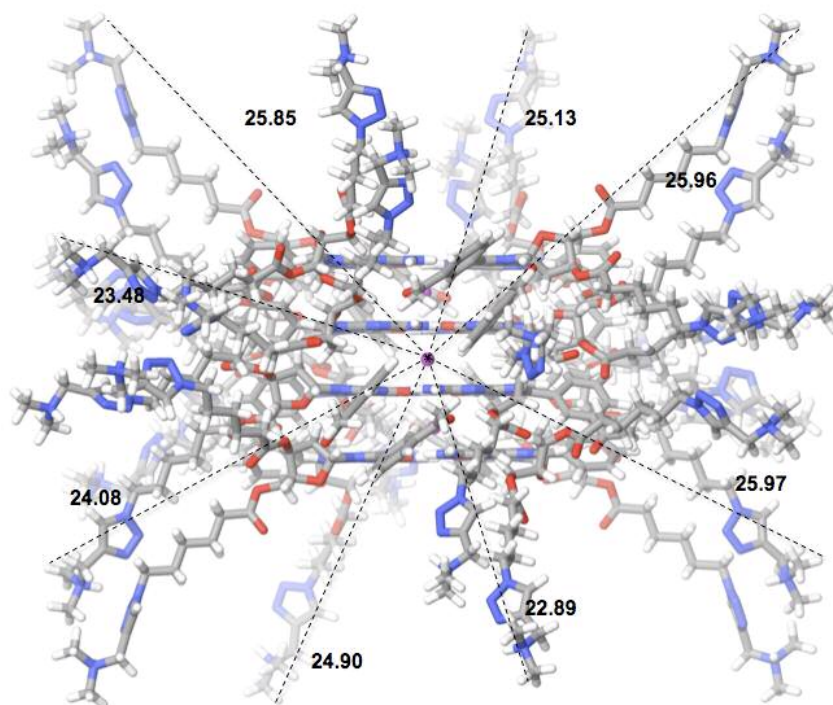


**Figure S26.** Hydrodynamic radii determined using a molecular model of  $(\text{mAGcat})_{16}\cdot 3\text{KCl}$  as created using AMBER\* (*MacroModel, Version 9.5, Maestro 8.0.315, Schrödinger, LLC, New York, NY, 2007*) representing water as a continuum solvent. The purple spheres represent potassium cations.

### **Variable temperature NMR**

A solution of **mAGcat** (10 mM) containing an excess of KCl (1 M) was placed in a threaded cap sealed NMR tube. The  $^1\text{H}$ -NMR was recorded in  $\text{H}_2\text{O}$ - $\text{D}_2\text{O}$  (9:1) at 25 °C and increased up to 80 °C, at 5 °C intervals. The fraction of ordered species was determined by the integration of the area under selected peaks ( $\text{H}^1$  in the monomer and hexadecamer) and reported as the ratio between the monomer and the G-quadruplex.

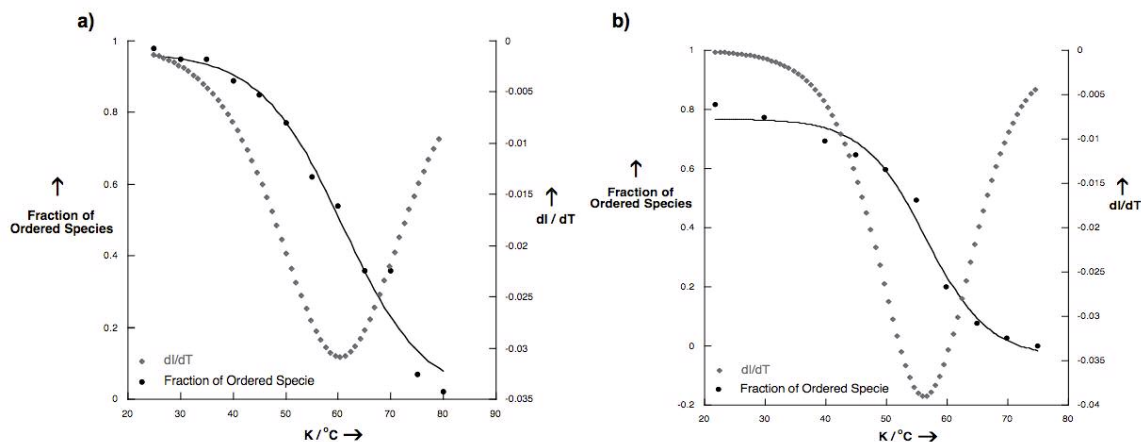


**Figure S27.** Melting curves of; a) **mAGcat** (10 mM), as determined by NMR by the fraction of ordered species (black line) measured at 1 M KCl in H<sub>2</sub>O-D<sub>2</sub>O (9:1). The first derivative plot of the melting curve is represented in dots; and b) **mAGi** (5 mM) in CD<sub>3</sub>CN saturated in KI. The first derivative plot of the melting curve is represented in dots.

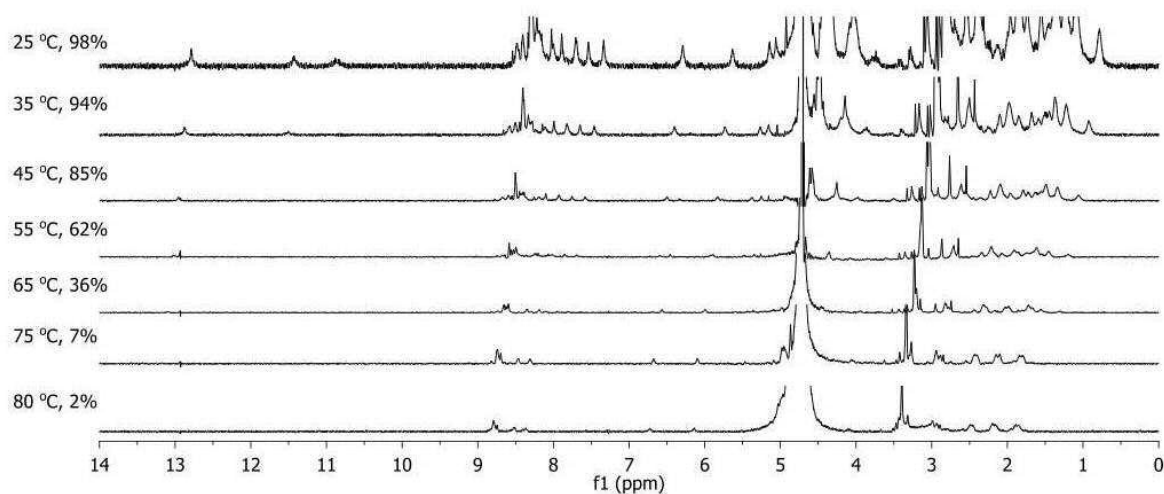


**Figure S28.** Variable temperature <sup>1</sup>H-NMR of **mAGcat** (10 mM), 1 M KCl in H<sub>2</sub>O-D<sub>2</sub>O (9:1), indicating the fraction of ordered species.

### **Differential Scanning Calorimetry (DSC)**

The total heat required for the dissociation of the hexadecamer was measured in water, in a temperature range of 20-90 °C, using a heating rate of 1 °C min<sup>-1</sup>. The  $T_m$  value is taken as the maxima in the DSC curve. Standard thermodynamic parameters were obtained from the DSC experiment using the relationships  $\Delta H_{\text{cal}} = \int \Delta C_P(T) dT$ ,  $\Delta S_{\text{cal}} = \int \Delta C_P(T)/T dT$  and the Gibbs equation,  $\Delta G_{\text{cal}}^0 = \Delta H_{\text{cal}} - T\Delta S_{\text{cal}}$ , where  $C_P$  is the heat capacity of the solution during the disassembly process.

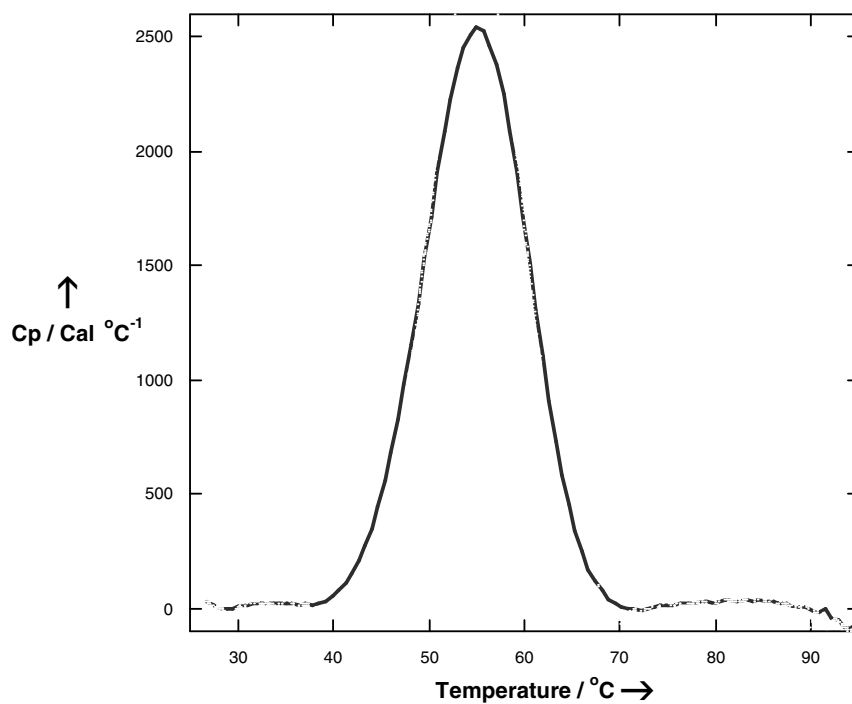


**Figure S29.** DSC melting curve of **mAGcat** (1 mM) in H<sub>2</sub>O with 1 M KCl.

**References:**

- 1) V. Gubala, J. E. Betacourt, J. M. Rivera, *Org. Letts.*, **2004**, *6*, 4735.
- 2) J. S. Moore, S. I. Stupp, *Macromolecules*, **1990**, *23*, 65.
- 3) C. Grandjean, A. Boutonnier, C. Guerrero, J.-M. Fournier, L. A. Mulard, *J. Org. Chem.*, **2005**, *70*, 7123.